Radiated Emissions Extrapolation Issues

by

Joshua Mack Martin

A thesis submitted to the Graduate Faculty of
Auburn University
in partial fulfillment of the
requirements for the Degree of
Master of Science

Auburn, Alabama
May 14, 2010

Keywords: electromagnetics, radiated emissions
extrapolation, log periodic

Approved by

Thomas Shumpert, Chair, Professor Emeritus of Electrical Engineering
Lloyd Riggs, Professor of Electrical Engineering
Michael Baginski, Associate Professor of Electrical Engineering

Abstract

In this thesis, the complicated problem of extrapolating radiated emissions from one range to another is tackled. A model employing a Method of Moments (MoM) formulation is presented to compare alongside measurements which had been previously completed in an OATS environment using a log periodic (LP) antenna as the source and an electric field probe to measure the radiated emissions. Measurements were performed at 3m and 10m ranges and varying heights. Results from the model are compared to the measured values to show the validity of the model. Finally, extrapolation of the measured data is presented and conclusions are made from the results.

Acknowledgements

The author would like to thank Dr. Thomas Shumpert for his patience and guidance throughout this entire process. Thanks also go to the Electromagnetic Environmental Effects branch of the Redstone Test Center for providing the facilities and equipment that made this project possible. Also, this project would not have been possible without the help of Jarrett Branch who was right there every step of the way as the measurements were made. Lastly, thanks go to all family members, friends, classmates, and professors who contributed with their love and support.

Table of Contents

List of Tables

List of Figures

CHAPTER 1

INTRODUCTION

1.1 Background and Motivation

Electromagnetic radiated emissions measurements are made for a wide variety of reasons. A widely used environment for making these measurements is known as an open air test site (OATS) [10]. While these measurements are made in an open area free of any scattering objects such as buildings or trees, there still remains the issue of the ground plane. While it is recommended in OATS testing that there be a wire ground place present of certain minimum dimensions associated with the maximum wavelength of testing, often OATS-type testing is done on smaller ground planes or even over actual ground (earth). Many times, measurements made in this OATS environment are made at distances other than that which is desired. These measurements then need to be extrapolated to the desired range. In these cases, this extrapolation is performed using an inverse linear-distance extrapolation factor of 1/R, where R is the distance from the source to the observation point. However, this extrapolation is not accurate in these cases with a ground plane present. The ground plane introduces interference which causes the radiated emissions to vary with many different factors such as polarization, frequency, height, etc. While predicting the fields over a ground plane is a very difficult issue in itself, the task of extrapolation of these fields from one distance to another is an even more complicated problem [11].

1.2 Outline

In this thesis, a model is developed and its results compared to detailed measurements at several ranges that had been previously completed. These measurements were performed in the summer of 2009 in an OATS environment using a log periodic (LP) antenna as the source and an electric field probe to measure the radiated emissions. These are shown in Figures 1.1 and 1.2 respectively. Measurements were performed at varying heights and distances of 3m and 10m which coincide with the FCC Emission Limits for Class B and Class A Digital Devices.

Figure 1.1: LP Antenna

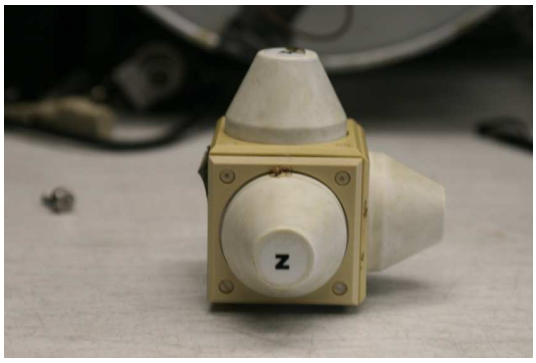

Figure 1.2: Electric Field Probe

Chapter 2 presents a detailed introduction to the model that was developed using a Method of Moments solution [1]. Also discussed is how the ground plane as well as the characteristics of the LP antenna was incorporated into the model. Next, Chapter 3 compares the experimentally obtained measurements to the values obtained from the model. Various approaches employed within the model as well as its self-consistency are also explained. Finally, in Chapter 4 the issue of field extrapolation is tackled as well as the results of extrapolation for the measured data.

CHAPTER 2

RADIATED EMISSIONS SOURCE MODEL

2.1 Introduction

In this chapter a model is presented and predicts the radiated fields from a log periodic (LP) antenna over a ground plane. This LP antenna will be modeled as a dipole of resonant length with augmented gain. Section 1 presents the development of the equations to solve for the current induced on the dipole. Section 2 outlines the procedure used in the development of a Method of Moments (MoM) solution. Section 3 presents the method for which the radiated fields are obtained from the dipole. The issue of accounting for the ground plane and the approach in the model for accounting for it are shown in Section 4. Finally, Section 5 outlines the reasoning for modeling the LP antenna as a simple resonant dipole.

2.2 Equation Development

In this section a mathematical model of a thin wire antenna is presented. First the magnetic vector potential in free space is derived [1]. The relationship between electric field and magnetic vector potential and electric scalar potential is given by:

$$E = -j\omega A - \nabla\phi \tag{2.1}$$

which can be expressed only in terms of A as:

$$E = -j\omega A - \frac{j}{\omega\mu\varepsilon}\nabla(\nabla \cdot A) \tag{2.2}$$

where A is the magnetic vector potential and ϕ is the electric vector potential.

Furthermore, the magnetic vector potential can be written in terms of the current J and the Green's Function $G(r,r')$ as:

$$A(r) = u\iiint J(r')G(r,r')dr' \tag{2.3}$$

where the Green's Function is defined as:

$$G(r,r') = \frac{e^{-jk|r-r'|}}{4\pi|r-r'|} \tag{2.4}$$

Now consider a perfectly conducting thin wire oriented in the $\hat{z}$-direction with a length L. The radius of the wire a is much less than L and λ. With the assumption that $L>>a$ there is negligible variation around the circumference of the wire; therefore, current only varies with respect to $\hat{z}$. The induced current on the wire is given by:

$$J_z(z) = \frac{I_z(z)}{2\pi a} \tag{2.5}$$

Expressing the current in terms of the magnetic vector potential,

$$A_z = \mu \int_{-L/2}^{L/2} I_z(z') \frac{e^{-jkr}}{4\pi r} dz' \tag{2.6}$$

and enforcing the boundary condition of zero tangential electric field on the surface of the wire yields:

$$E_z^{incident} + E_z^{scattered} = 0 \tag{2.7}$$

Substituting Equation (2.7) into Equation (2.2) and enforcing the boundary condition one obtains the solution for the electric field on the wire:

$$E_z^{i} = \frac{j}{\omega\varepsilon} \int_{-L/2}^{L/2} I_z(z') \left[\frac{\partial^2}{\partial z^2} + k^2 \right] \frac{e^{-jkr}}{4\pi r} dz' \tag{2.8}$$

where the distance from the source to the observation point r is given by:

$$r = \sqrt{(z - z')^2 + a^2} \tag{2.9}$$

Equation (2.8) is known as Pocklington's Integral Equation.

2.3 Solving for Current

Pocklington's Integral Equation is solved for the current along the wire using a Method of Moments (MoM) approach [2]. This technique involves breaking the wire into small segments and solving for the current on each segment.

In order to model this wire as a simple radiating dipole antenna, a delta-gap source (Figure 2.1) is used to model a voltage applied between the antenna terminals. It can be expressed as:

$$E^i = \frac{V_o}{\Delta z}\hat{z} \tag{2.10}$$

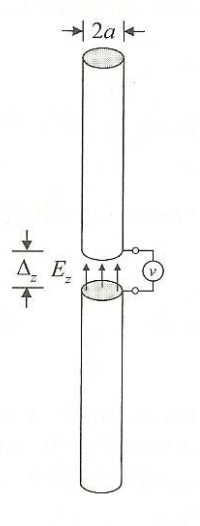

Figure 2.1: Illustration of a Delta Gap Source

For this model, the desired voltage is applied across the center section of the wire. The voltage is set to zero for all other segments. With this in place, the current can be calculated along the wire driven by a delta-gap voltage source.

2.4 Solving for Fields

With the currents calculated, one can solve for the radiated fields due to the induced current along the wire. The electric field components for a dipole in the z-direction are given by:

$$E_r = \frac{I\Delta z}{2\pi} e^{-jkr}\left(\frac{\eta}{r^2} + \frac{1}{j\omega\varepsilon r^3}\right)\cos\theta \tag{2.11}$$

$$E_\theta = \frac{I\Delta z}{4\pi} e^{-jkr}\left(\frac{j\omega\mu}{r} + \frac{\eta}{r^2} + \frac{1}{j\omega\varepsilon r^3}\right)\sin\theta \tag{2.12}$$

where I is the current value, Δz is the length of each wire segment length, r is the distance between the wire element and the observation point, and θ is the angle between the wire and the observation point [3].

To calculate the total field at a specified point the fields due to each individual current element are added together to obtain the total field.

For this model, the field component of interest is in the direction of the wire or the z-direction. It can be obtained by the following expression:

$$E_z = E_\theta \cdot \sin\theta \tag{2.13}$$

2.5 Ground Plane

Up to this point, the numerical model is applicable for free space; however, the ground plane is introduced to represent the surface of the earth. The approach to solving this issue is to employ image theory and Fresnel reflection coefficients [4]. The model also will take into account the orientation of the dipole. The two cases that will be considered are vertical and horizontal polarization of the dipole with respect to the ground plane as shown in Figure 2.2 and Figure 2.3.

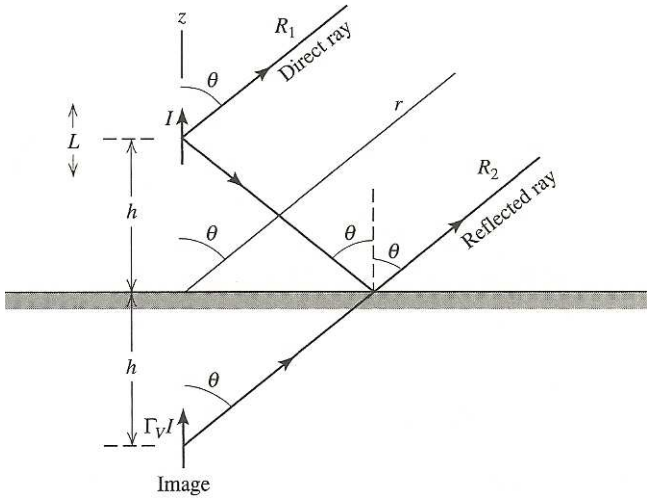

Figure 2.2: Vertical Polarization

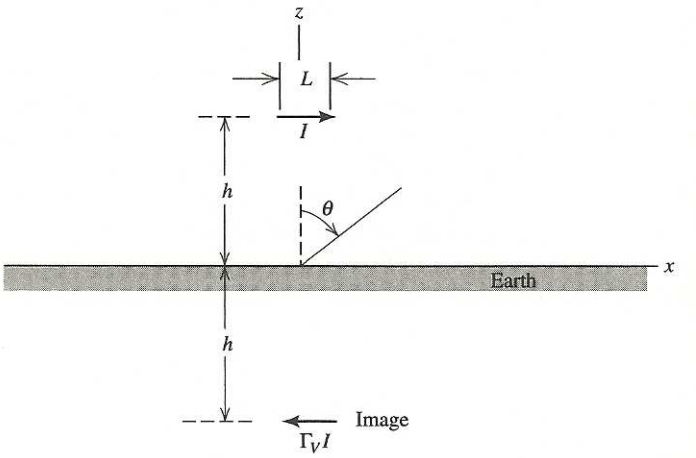

Figure 2.3: Horizontal Polarization

For each case, the image dipole must be accounted for with a Fresnel reflection coefficient. For the vertical case, this coefficient is defined by Equation (2.14) and for the horizontal case Equation (2.15) respectively [4].

$$\Gamma_V = \frac{\varepsilon'_r \cos\theta - \sqrt{\varepsilon'_r - \sin^2\theta}}{\varepsilon'_r \cos\theta + \sqrt{\varepsilon'_r - \sin^2\theta}} \tag{2.14}$$

$$\Gamma_H = \frac{\cos\theta - \sqrt{\varepsilon'_r - \sin^2\theta}}{\cos\theta + \sqrt{\varepsilon'_r - \sin^2\theta}} \tag{2.15}$$

where ε'_r is the relative permittivity of the ground and θ is the angle between the wire and the observation point.

A value of relative permittivity needs to be chosen to accurately represent the ground plane made of asphalt/soil. Long term research shows the permittivity of fresh asphalt to be as low as 3 [6]. The conductivity of the asphalt is negligible. Over time as the asphalt dries the permittivity rises up to the 5 to 7 range and remains there for the life of the asphalt before it breaks down. Given this evidence, a value of relative permittivity of 6 is chosen for the model.

An issue to be considered when selecting the reflection method is the interaction between the dipole and the ground plane for the horizontal case. From a study by Sarkar and Strait [8] it is shown that the results from the reflection method and the exact Sommerfield formulation was within ten percent as long as the dipole was at least a distance given by Equation (2.16) above the ground plane.

$$\frac{0.25}{\sqrt{\varepsilon_r}\lambda} \tag{2.16}$$

For the frequency range of interest and antenna dimensions it was determined that for the worse case scenario, the dipole to ground plane distance was well above this limit. Therefore, the conclusion was made that using image theory along with refection coefficients is a reasonable approximation.

With the ground plane now taken into account, the total field is defined as the field from the dipole plus the field from the image dipole multiplied by the appropriate reflection coefficient.

2.6 Log Periodic Antenna Approximation

A log periodic (LP) antenna is a broadband antenna composed of different dipoles of varying lengths. It has been proven that with changes of frequency the active region or phase center of the LP antenna is also changing. It has been shown that the radiated energy from a LP antenna comes from the active region [5]. This active region is essentially composed of the dipole of resonant length plus the nearest element to either side of the resonant element. The resonant length of a dipole is approximately equal to one-half of a wavelength.

Therefore, this LP antenna will be represented as a dipole of resonant length. Using the dimensions of the actual LP antenna being modeled (shown in Table 2.1), the position of the dipole in the model is adjusted with changing frequency to account for the shifts in the active region.

In the actual LP antenna, the presence of adjacent elements account for additional gain with the longer elements acting as reflectors and the shorter elements acting as directors. This enhanced gain is accounted for in the MoM model by employing an augmented gain based on the measured fields from the actual LP antenna at unique observation points associated with the approximate Brewster angle of incidence [7].

Element	Length (m)	Resonant Frequency (MHz)	Lateral Offset (m)
1	1.71	88	2.05
2	1.47	100	1.83
3	1.35	111	1.59
4	1.20	125	1.42
5	1.07	140	1.24
6	0.95	158	1.10
7	0.86	175	0.98
8	0.75	200	0.86
9	0.67	224	0.76
10	0.59	255	0.67
11	0.54	281	0.59
12	0.47	321	0.51
13	0.43	350	0.45
14	0.37	400	0.39
15	0.35	432	0.34
16	0.29	510	0.30
17	0.27	561	0.26
18	0.23	660	0.22
19	0.21	701	0.19
20	0.19	802	0.16
21	0.17	863	0.13
22	0.14	1069	0.11
23	0.13	1122	0.09
24	0.12	1247	0.07

Table 2.1: Physical Dimensions of the LP Antenna

It should be noted that for the frequencies of 150, 250, and 300 MHz there was not an element at that exact frequency; therefore, the lateral offsets were interpolated as 1.18, 0.68, and 0.55m respectively.

CHAPTER 3

EXPERIMENTALLY MEASURED RADIATED FIELDS AND COMPARISON OF MODEL AND MEASUREMENTS

3.1 Introduction

In this chapter measured data is compared against the results from the mathematical model. Section 3.2 graphically shows the comparison of measured to model data for all cases. In Section 3.3, the experimental setup is explained and the approach to taking the measurements that were obtained experimentally is presented. Next is an attempt to explain the comparisons along with a discussion of the self-consistency of the model in Section 3.4. Several methods are presented including utilizing Brewster's angle for the vertical polarization. Finally, in Section 3.5 it is explained how the measured values are matched against the model results including how the measured data was scaled by the driving point voltage of the model.

3.2 Presentation of the Comparison of Measured and Modeled Data

Figures 3.1-3.14 highlight the modeled data plotted against the measured results obtained experimentally for the 3m and 10m ranges for both horizontal and vertical polarization. While no measurements were taken at the 30m range, results of the model are included for this distance. (All normalizations of the measured data and the scaling of the model data are discussed in detail in later sections of this chapter.)

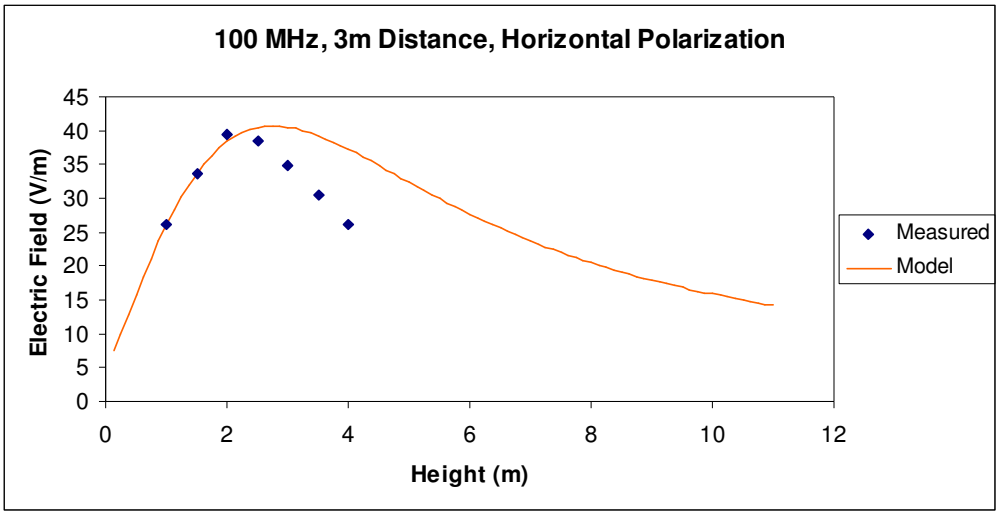

(a)

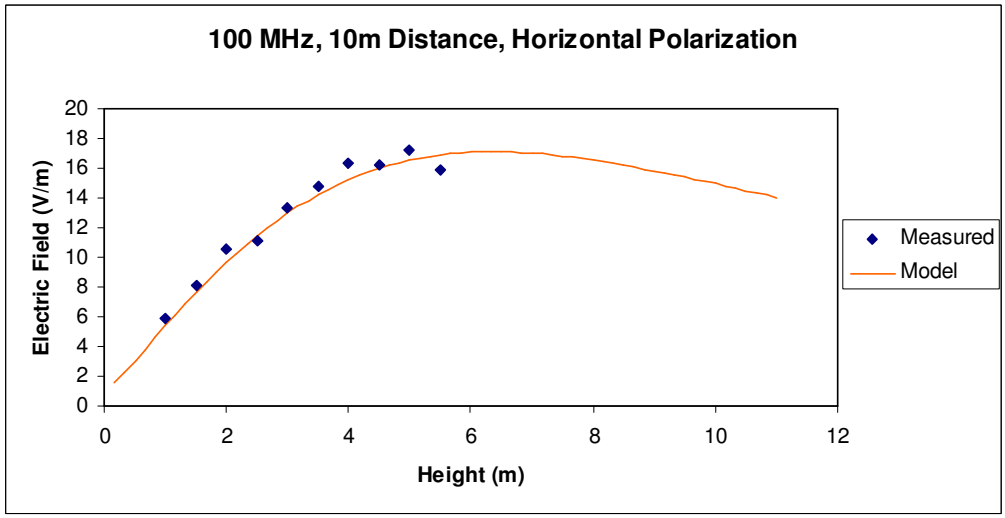

(b)

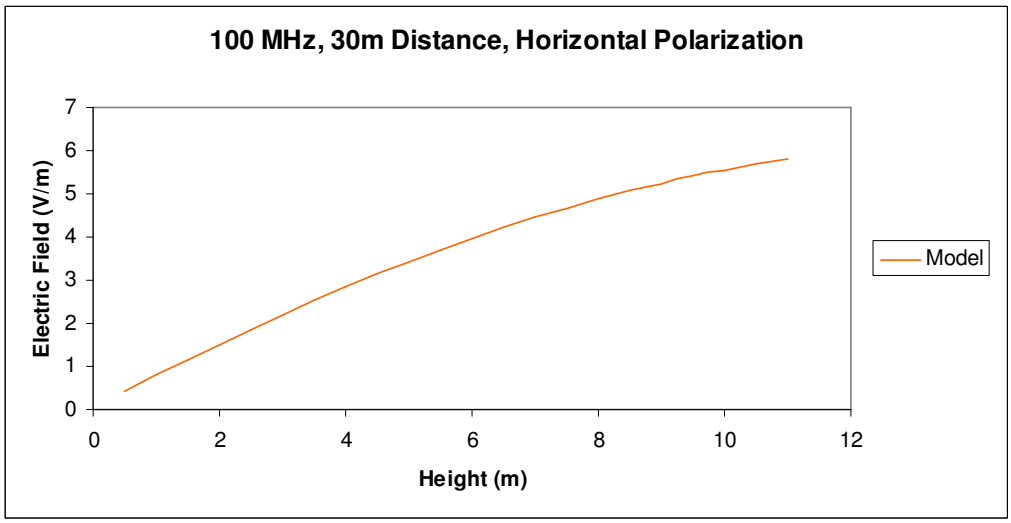

(c)

Figure 3.1: Horizontal Polarization at 100 MHz at (a) 3m (b) 10m and (c) 30m distances

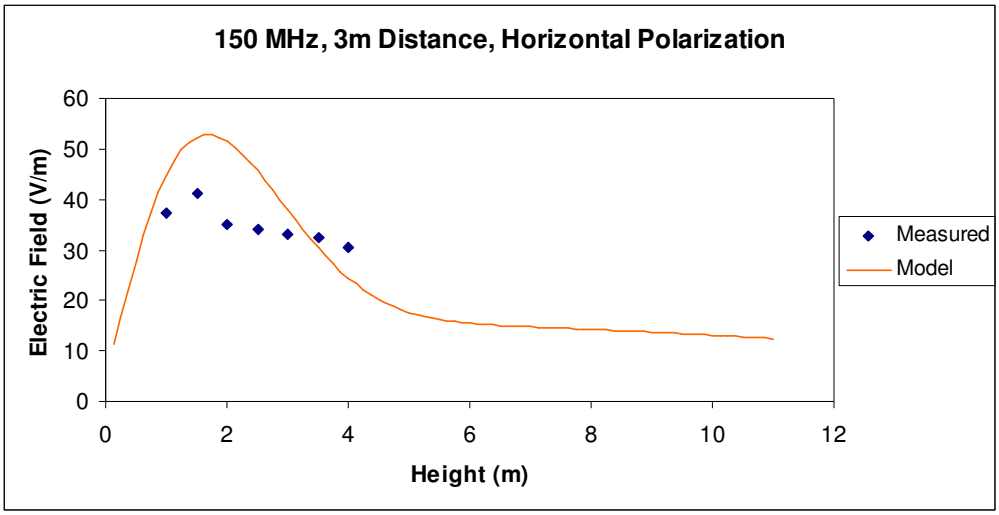

(a)

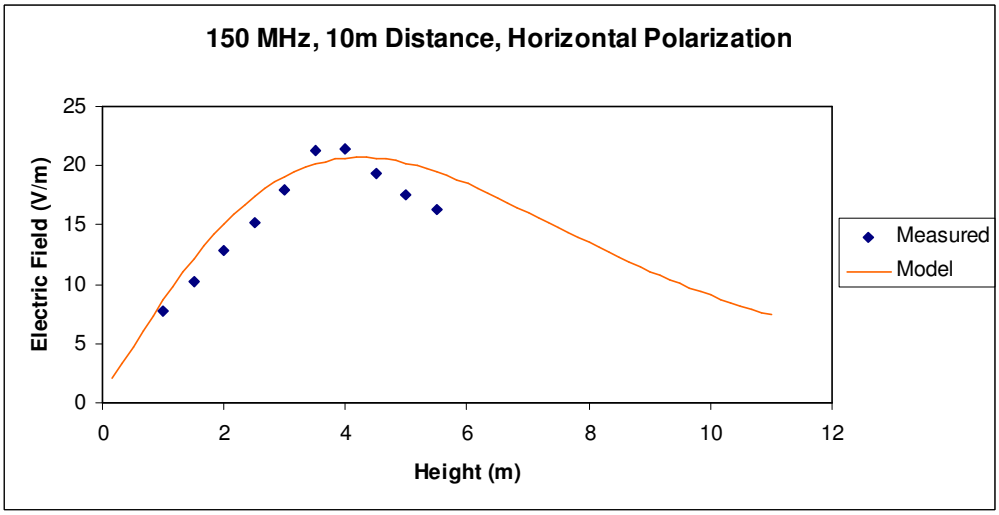

(b)

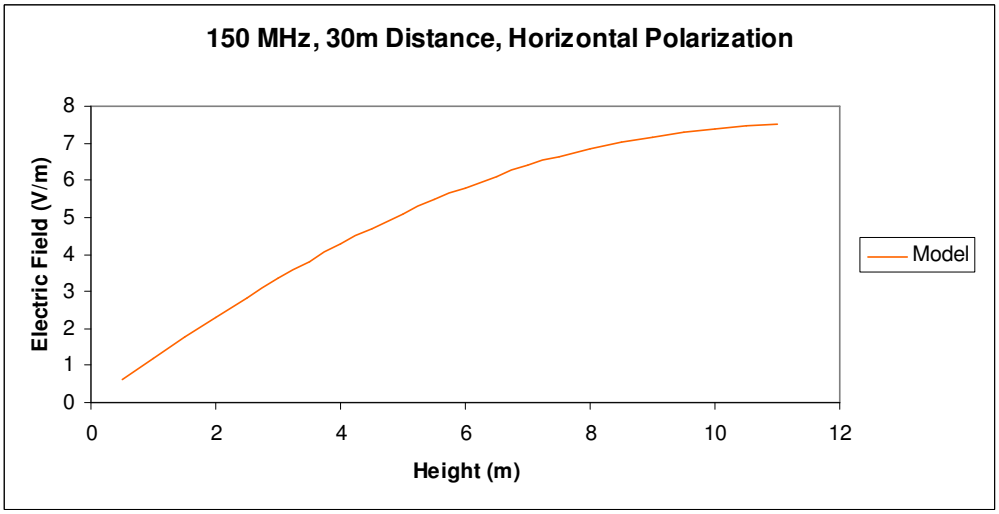

(c)

Figure 3.2: Horizontal Polarization at 150 MHz at (a) 3m (b) 10m and (c) 30m distances

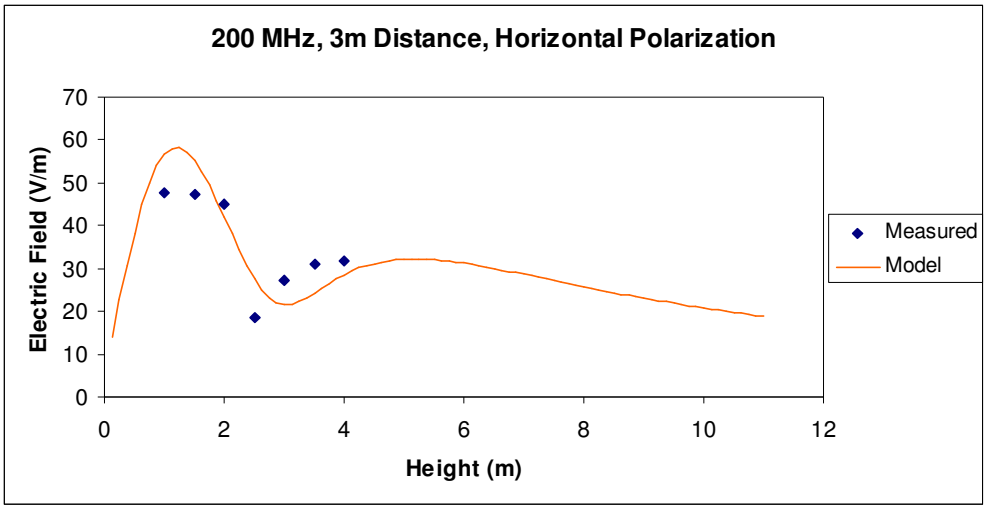

(a)

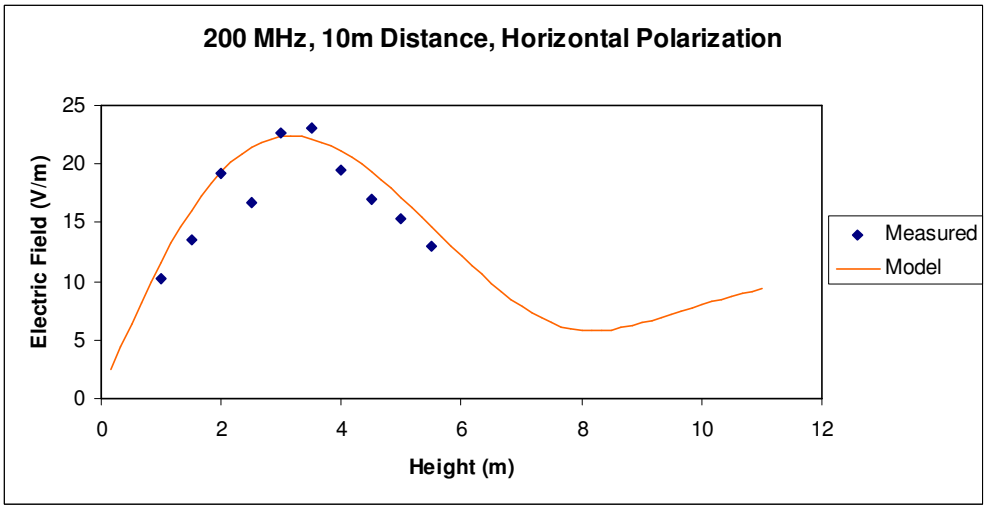

(b)

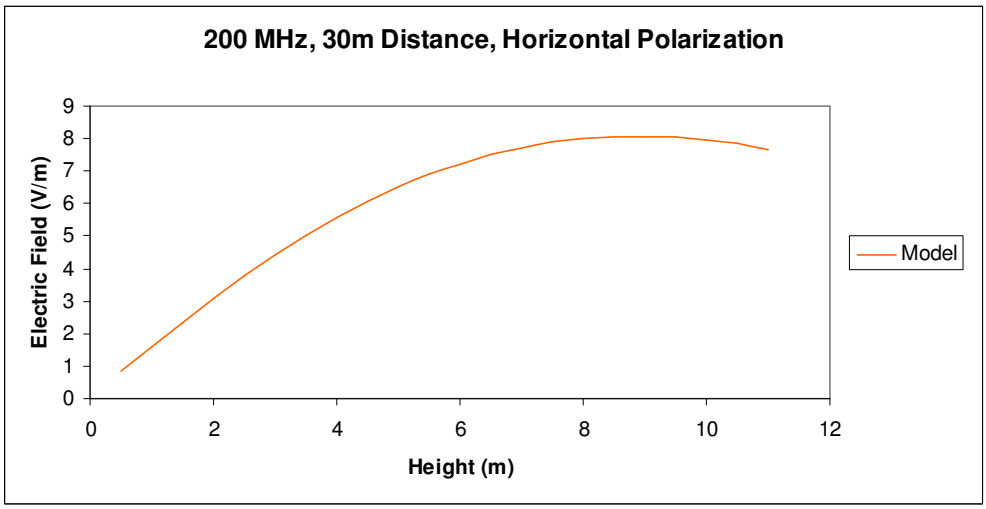

(c)

Figure 3.3: Horizontal Polarization at 200 MHz at (a) 3m (b) 10m and (c) 30m distances

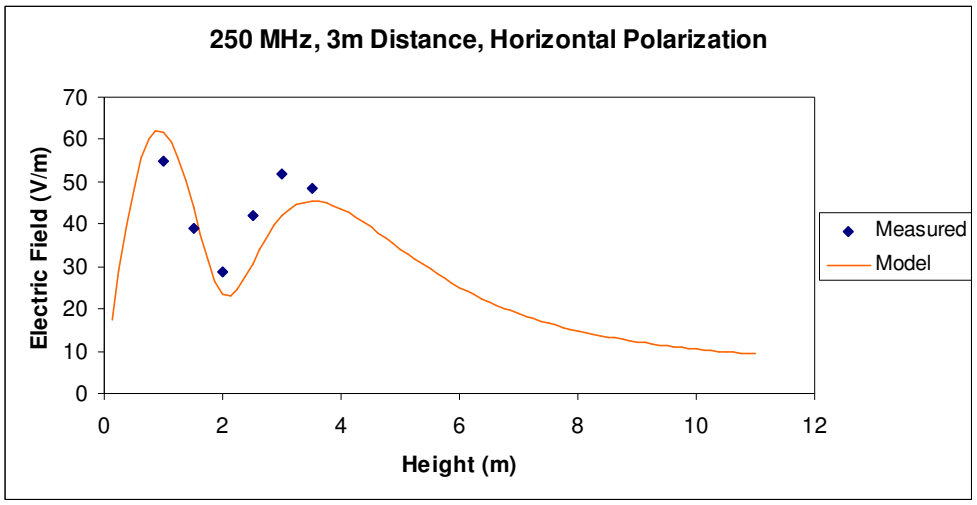

(a)

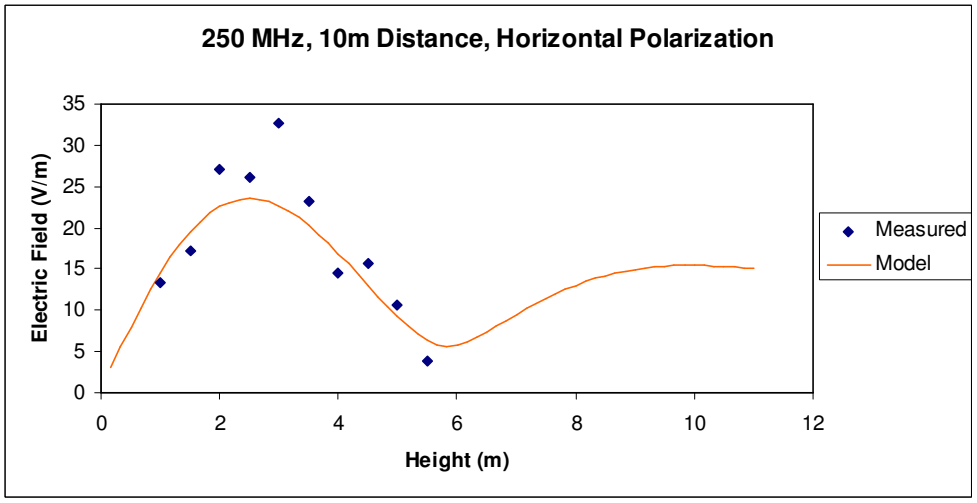

(b)

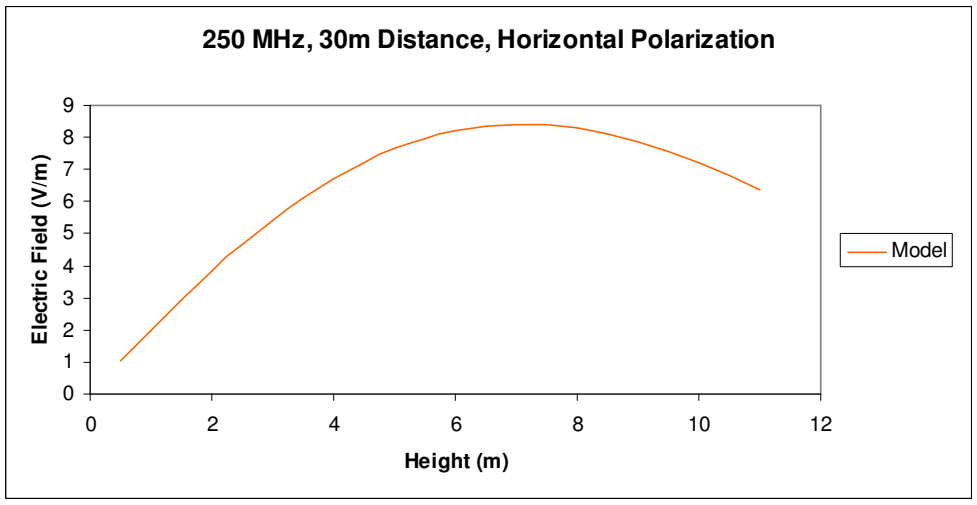

(c)

Figure 3.4: Horizontal Polarization at 250 MHz at (a) 3m (b) 10m and (c) 30m distances

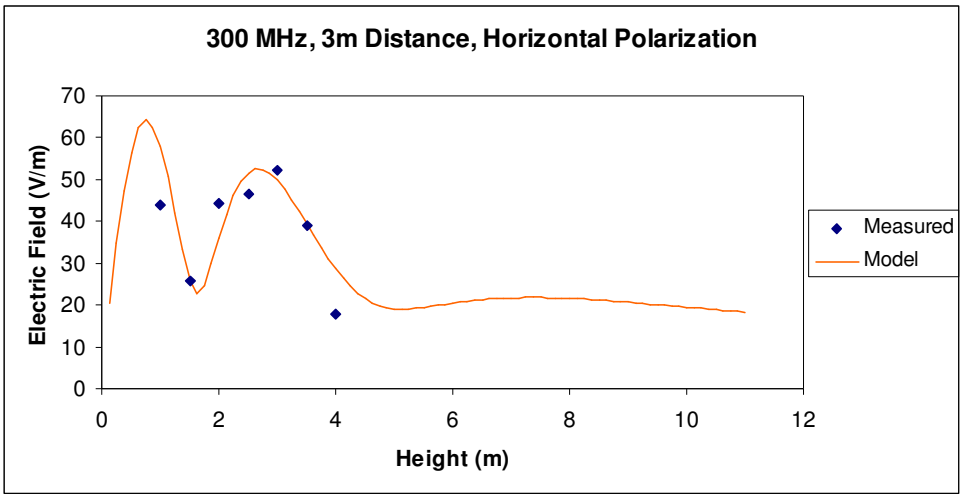

(a)

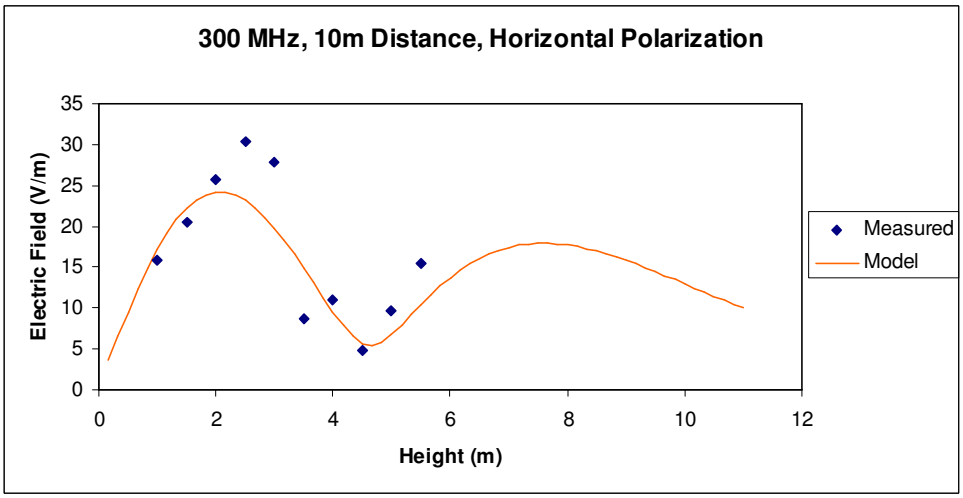

(b)

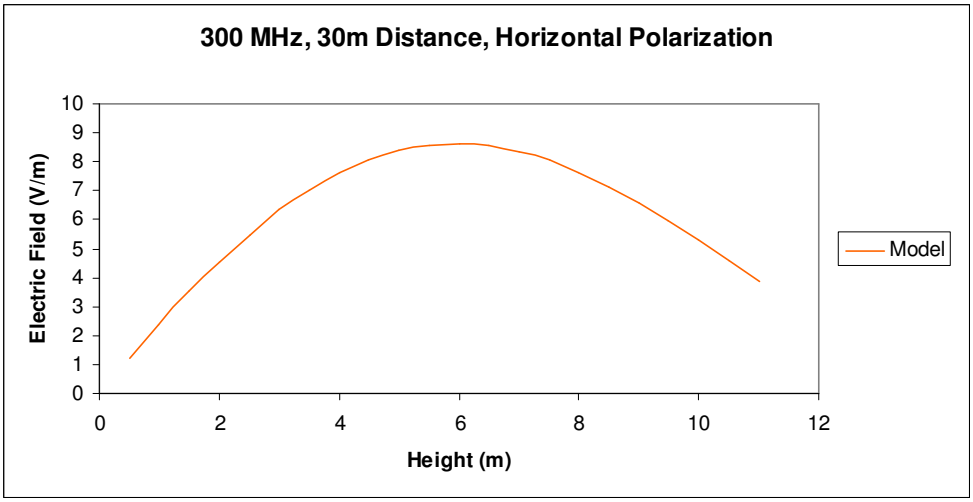

(c)

Figure 3.5: Horizontal Polarization at 300 MHz at (a) 3m (b) 10m and (c) 30m distances

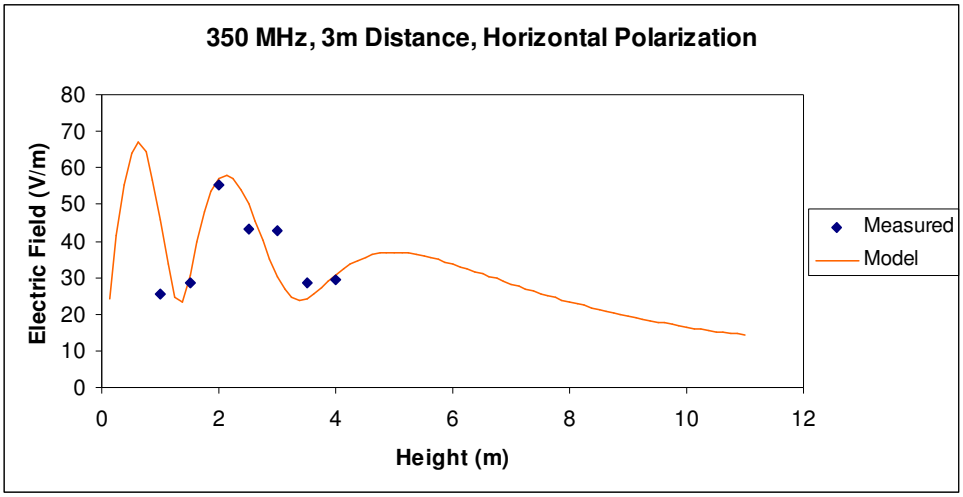

(a)

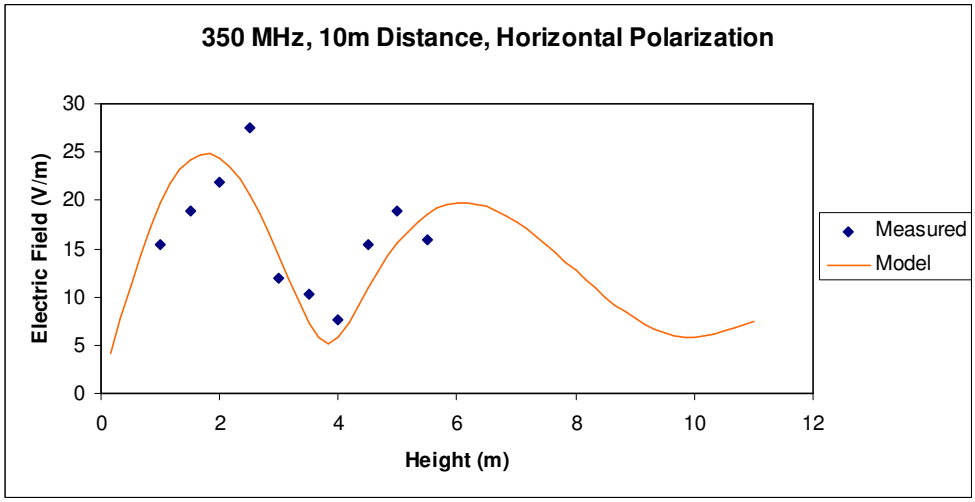

(b)

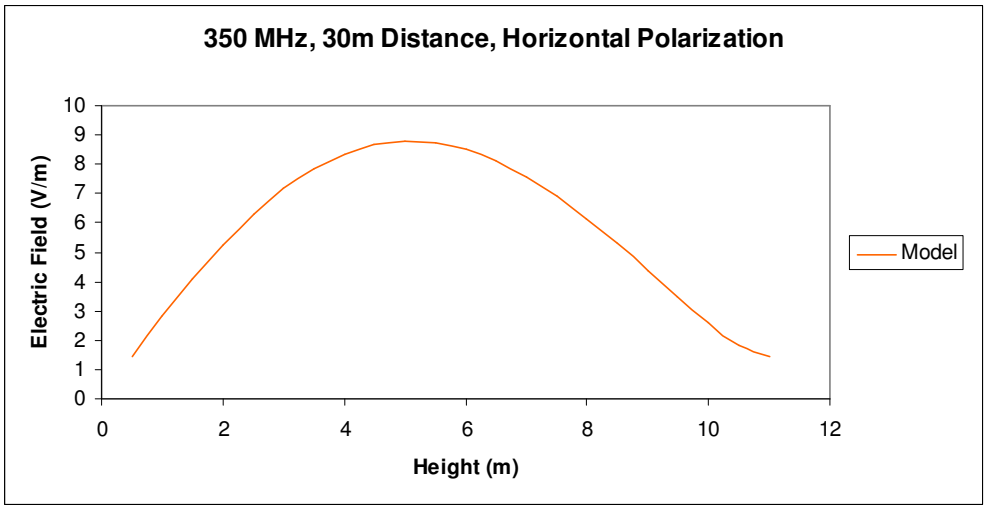

(c)

Figure 3.6: Horizontal Polarization at 350 MHz at (a) 3m (b) 10m and (c) 30m distances

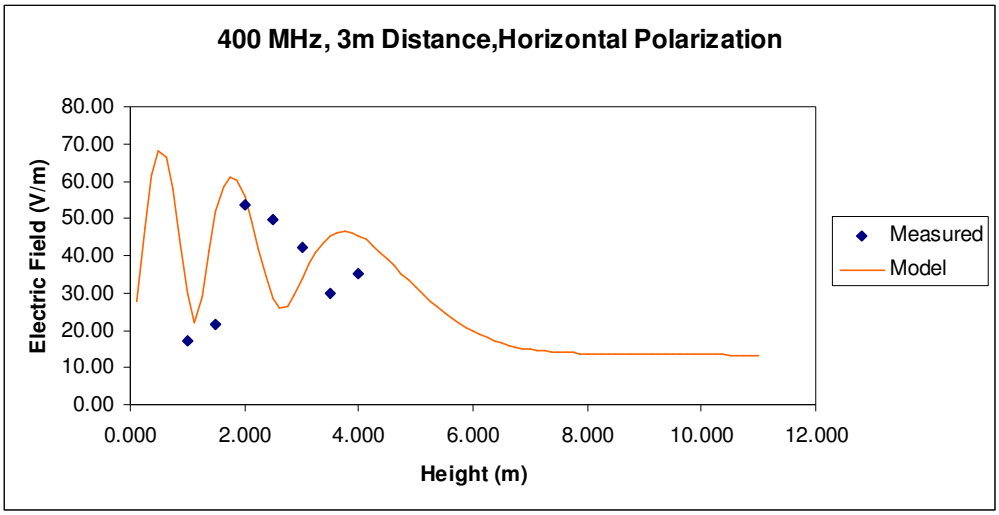

(a)

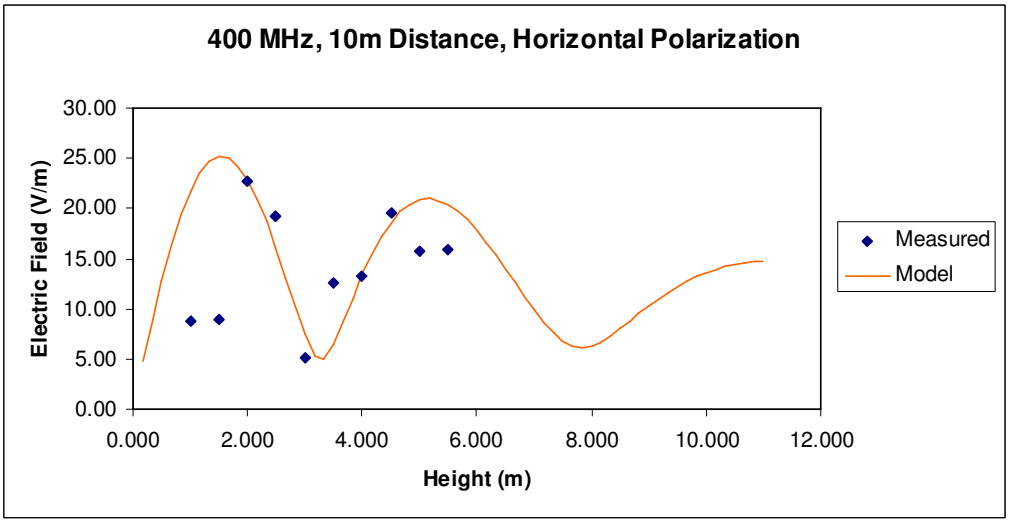

(b)

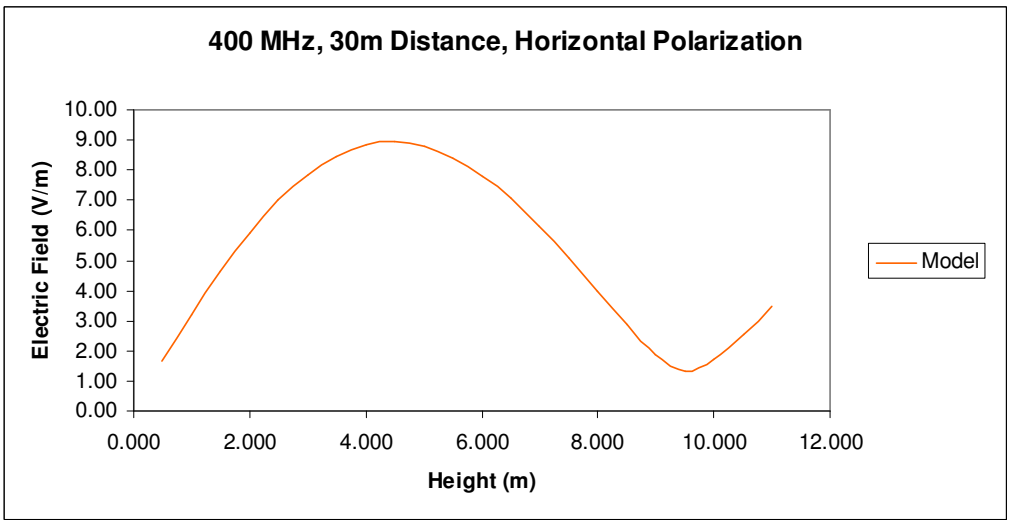

(c)

Figure 3.7: Horizontal Polarization at 400 MHz at (a) 3m (b) 10m and (c) 30m distances

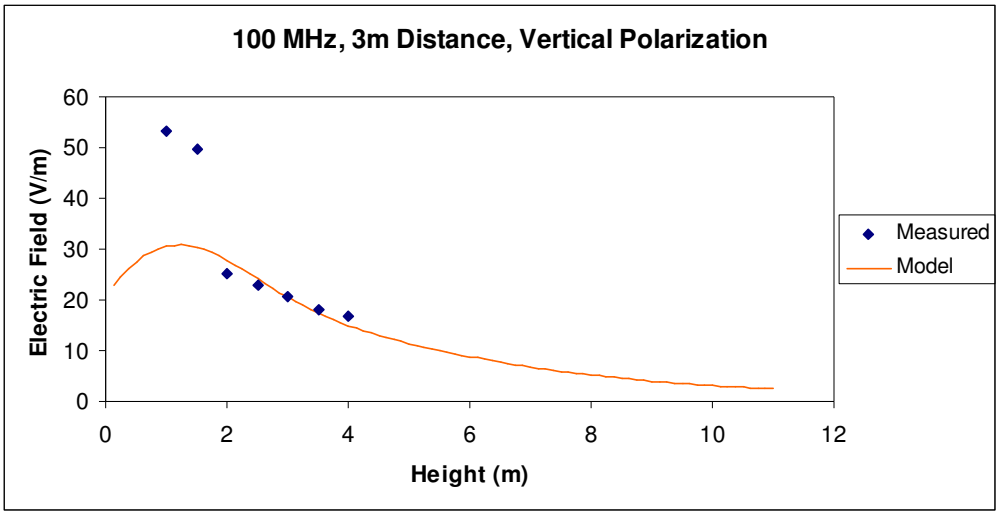

(a)

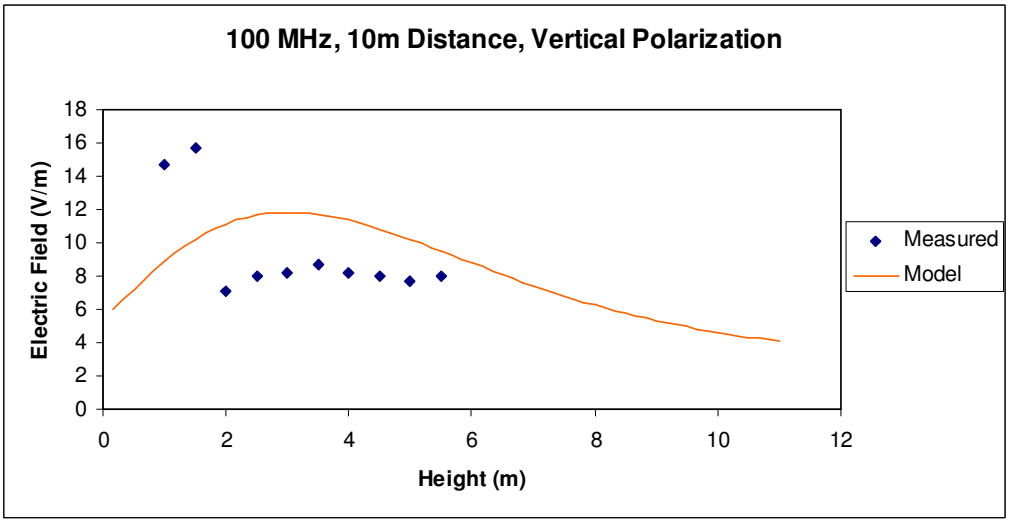

(b)

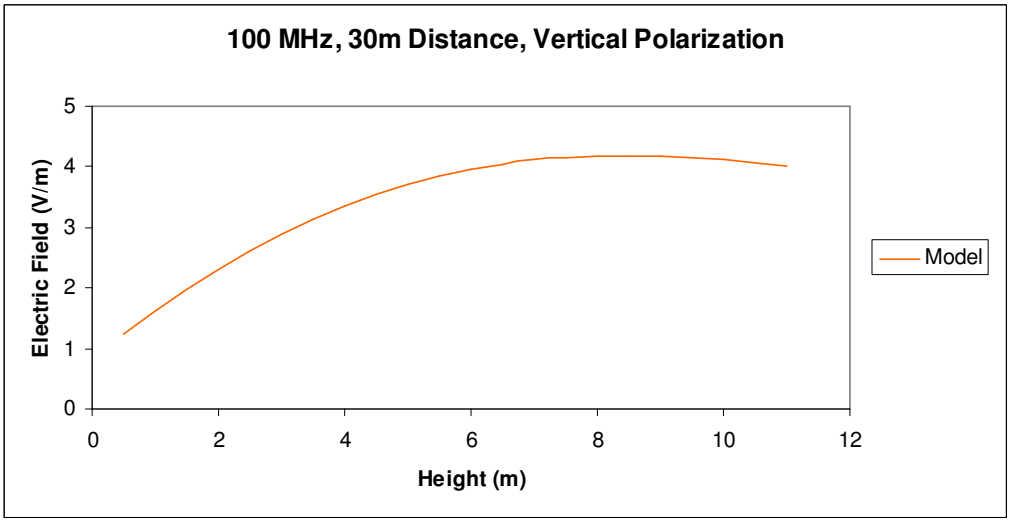

(c)

Figure 3.8: Vertical Polarization at 100 MHz at (a) 3m (b) 10m and (c) 30m distances

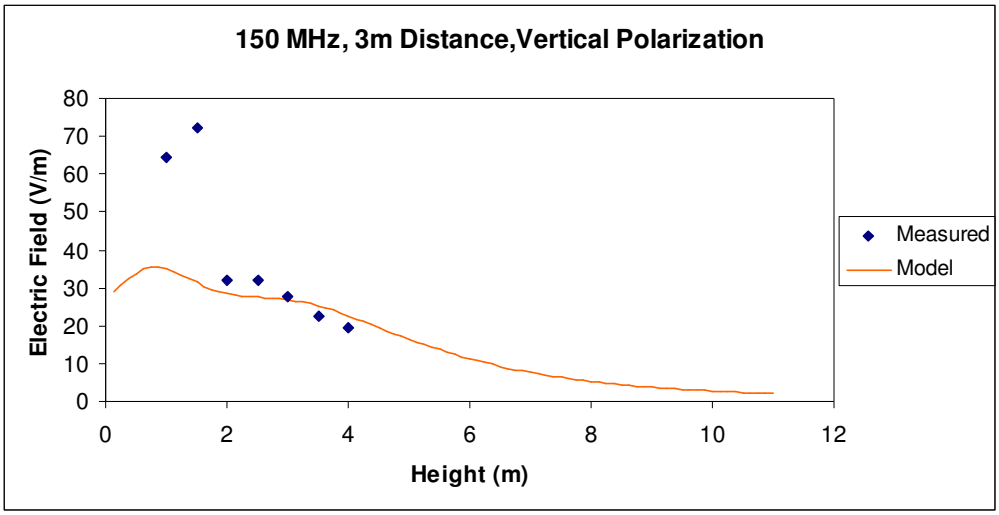

(a)

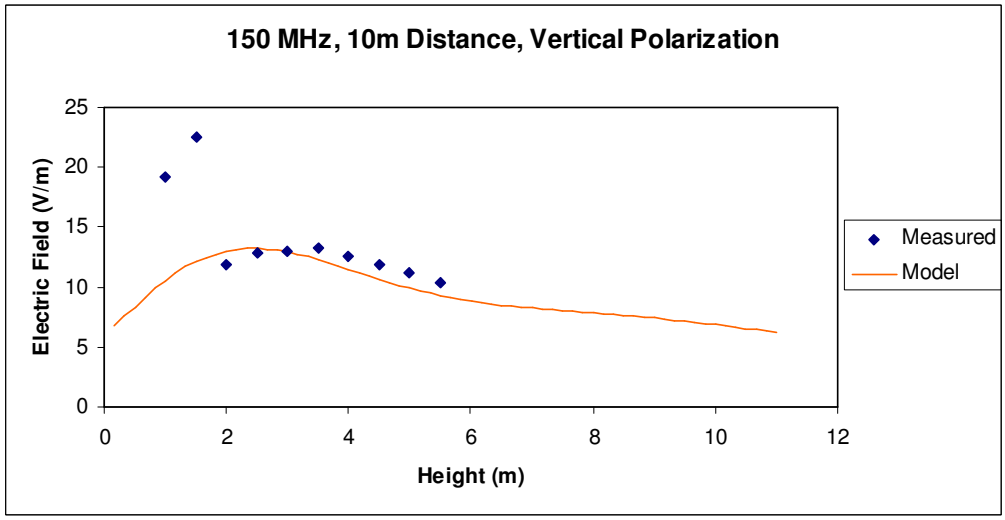

(b)

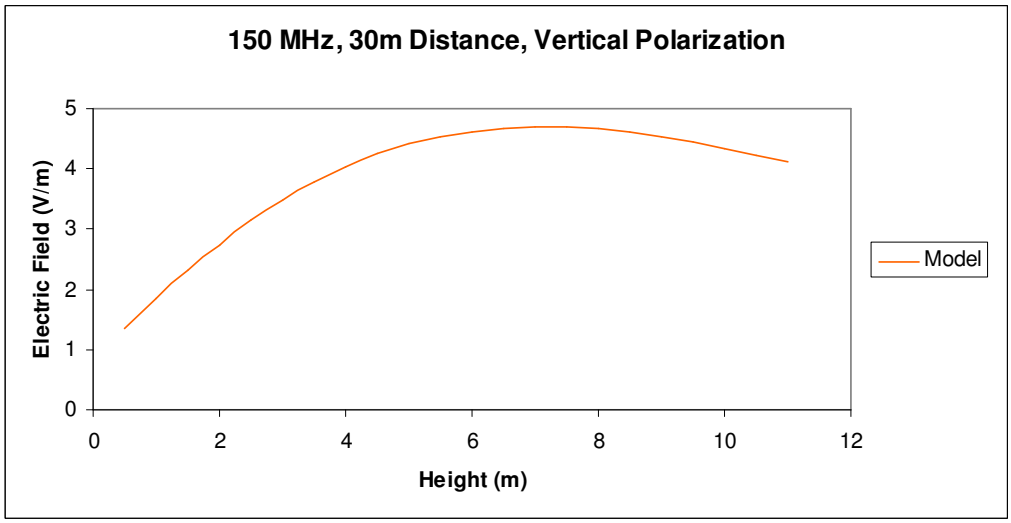

(c)

Figure 3.9: Vertical Polarization at 150 MHz at (a) 3m (b) 10m and (c) 30m distances

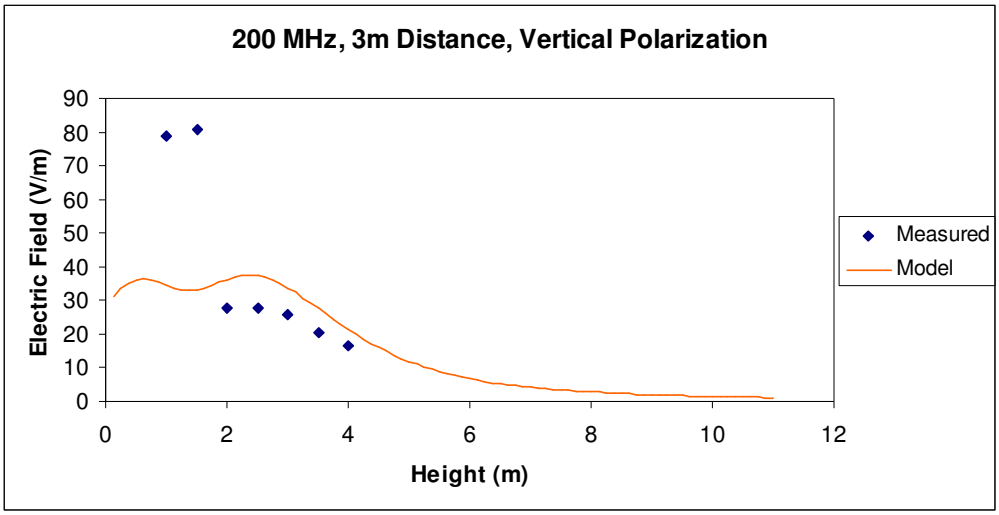

(a)

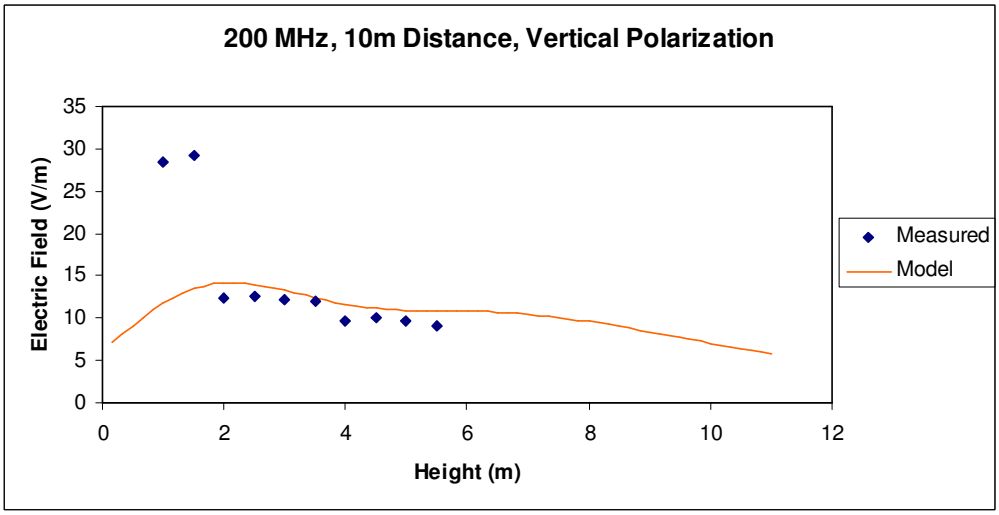

(b)

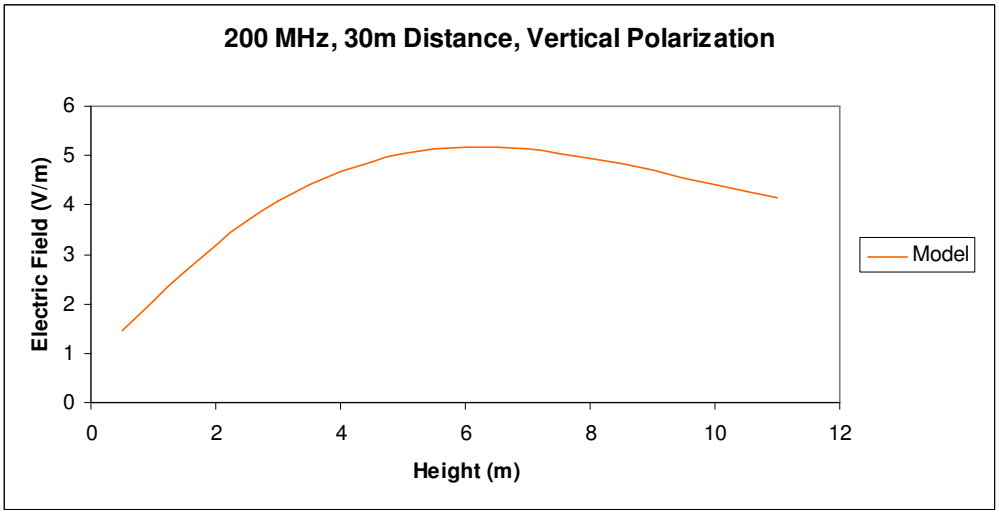

(c)

Figure 3.10: Vertical Polarization at 200 MHz at (a) 3m (b) 10m and (c) 30m distances

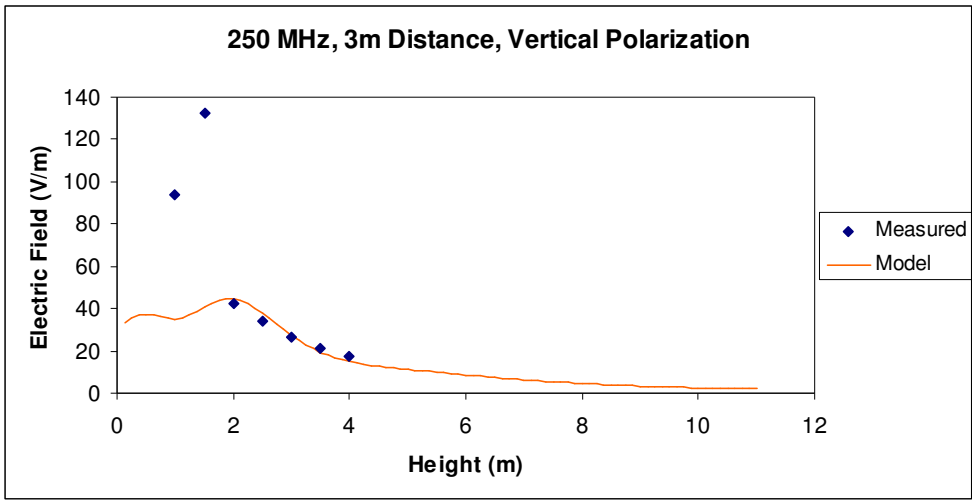

(a)

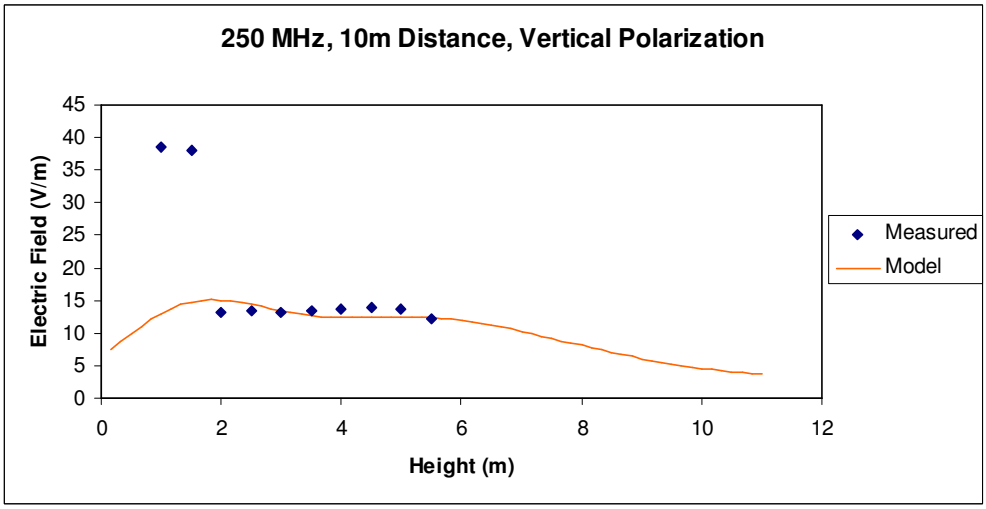

(b)

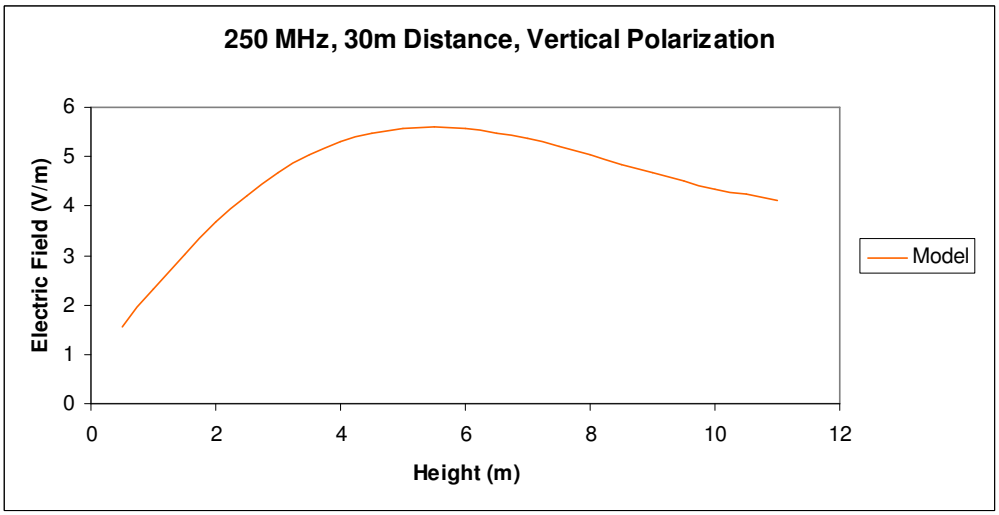

(c)

Figure 3.11: Vertical Polarization at 250 MHz at (a) 3m (b) 10m and (c) 30m distances

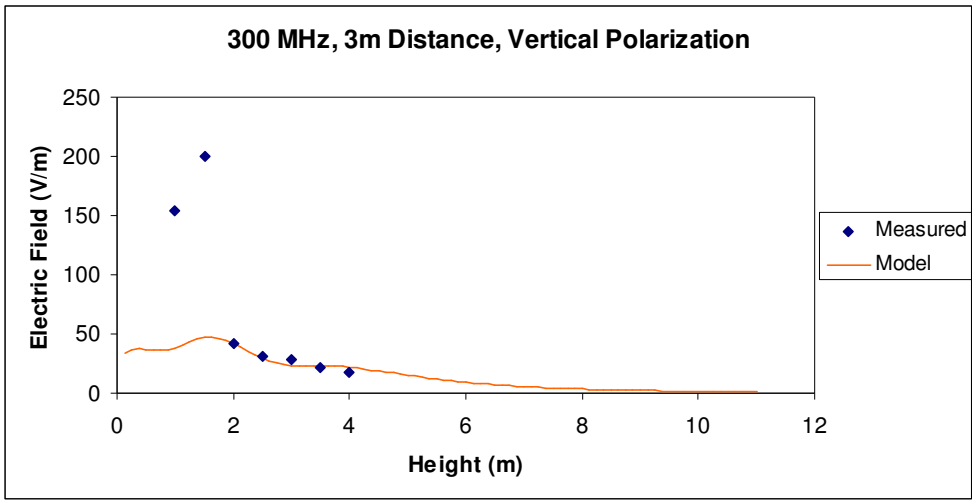

(a)

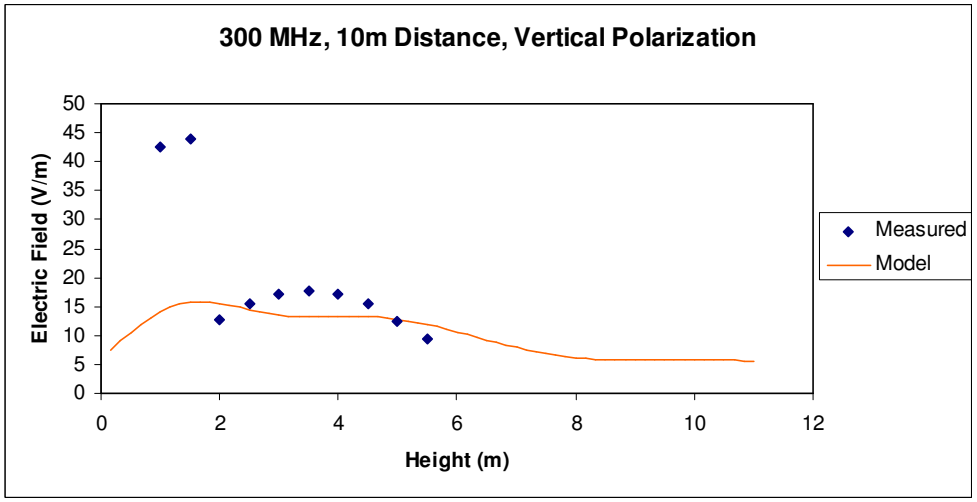

(b)

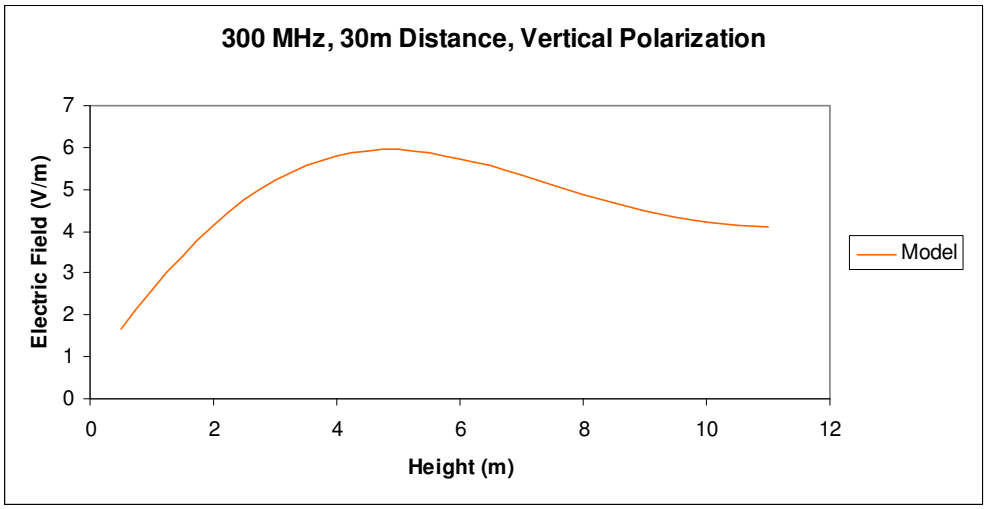

(c)

Figure 3.12: Vertical Polarization at 300 MHz at (a) 3m (b) 10m and (c) 30m distances

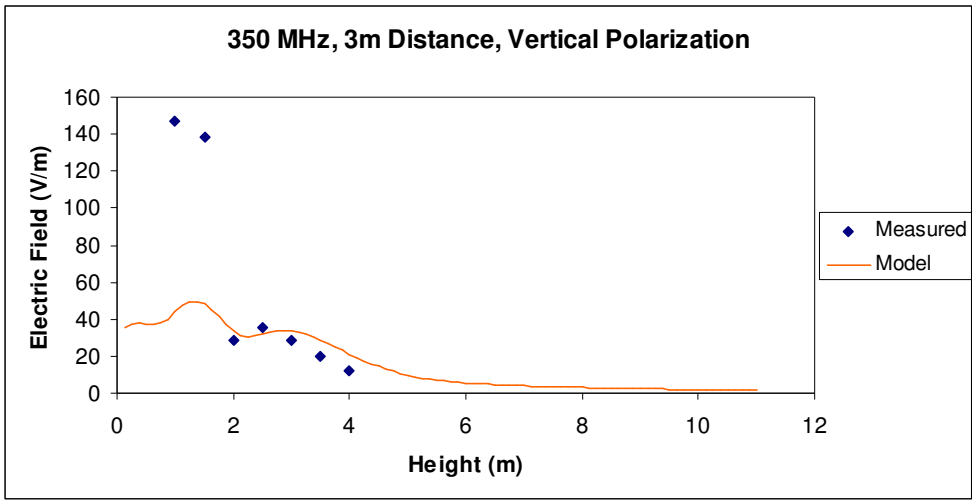

(a)

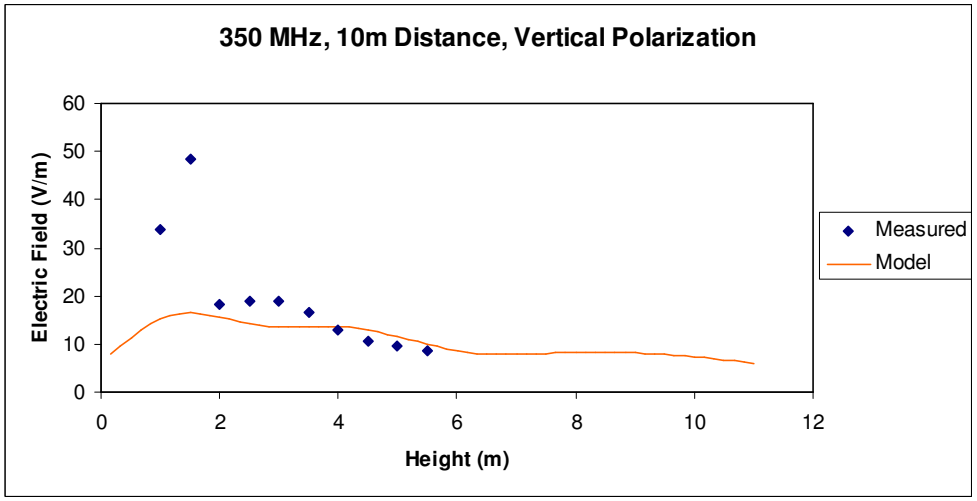

(b)

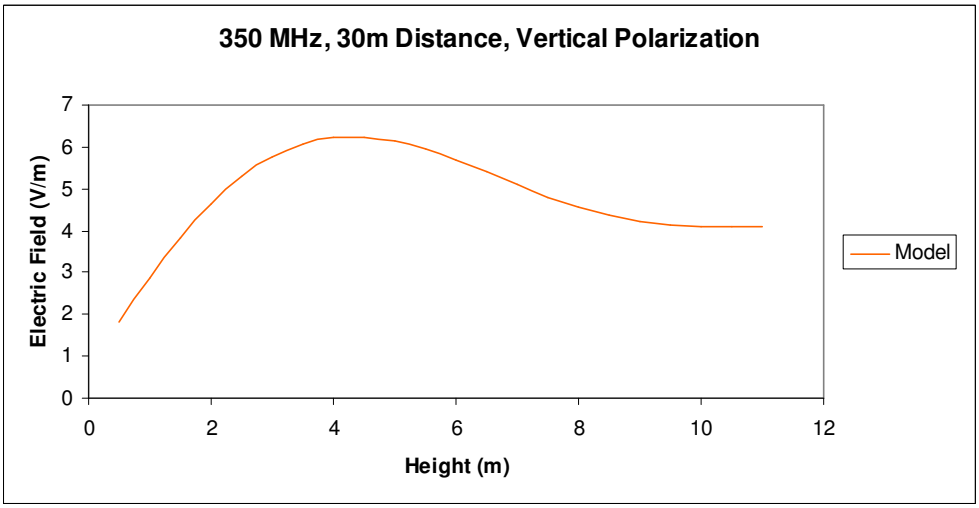

(c)

Figure 3.13: Vertical Polarization at 350 MHz at (a) 3m (b) 10m and (c) 30m distances

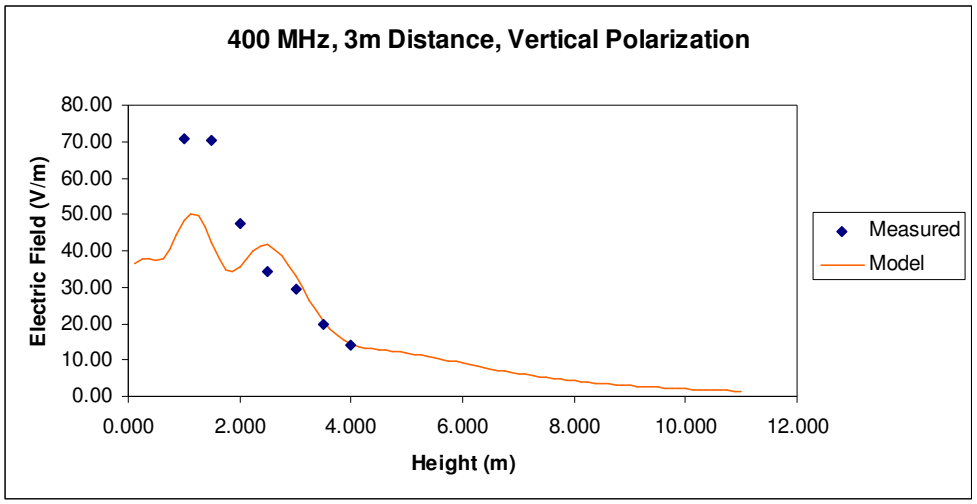

(a)

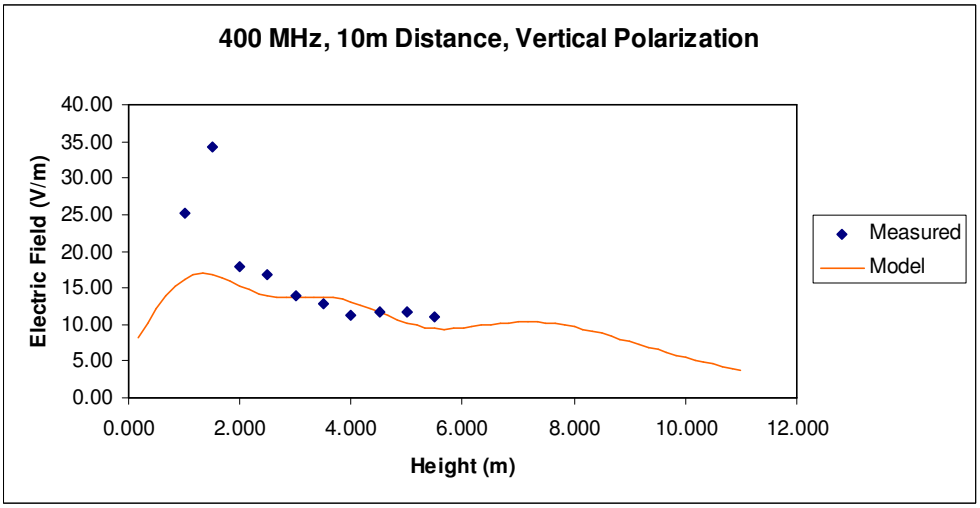

(b)

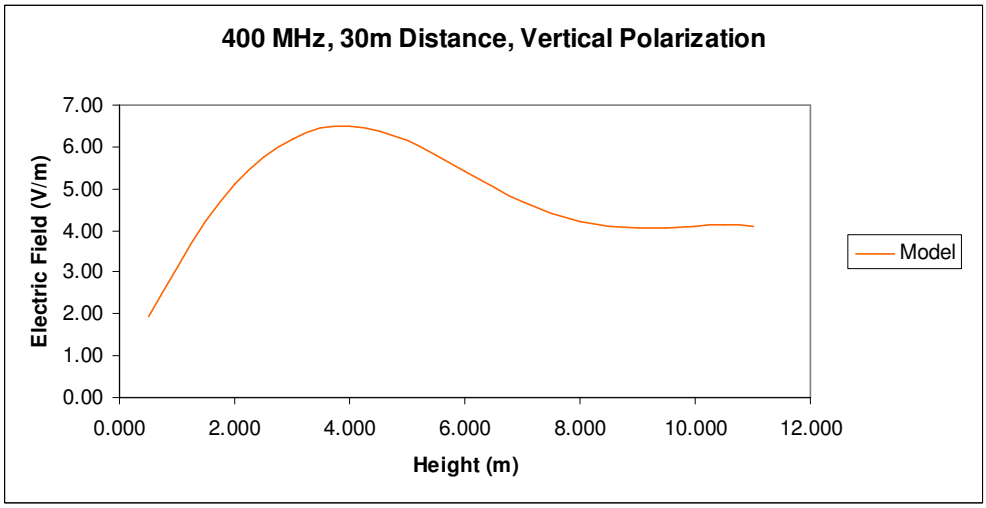

(c)

Figure 3.14: Vertical Polarization at 400 MHz at (a) 3m (b) 10m and (c) 30m distances

3.3 Setup for the Experiment Measurements

The motivation and goal behind performing the physical measurements was to take a transmitting antenna and measure the electric field at unique observation points. A log periodic (LP) antenna was chosen for the transmitting source and an electric field probe was employed to measure the radiated fields. Given the design characteristics of the LP antenna, the frequency range of interest was chosen to be 100 to 400 MHz with 50 MHz increments. The central height of the LP antenna was 1.25m above the ground plane. The actual ground plane was composed of an asphalt strip approximately 6m wide with typical Alabama earth below. All measurements were made in an open area many wavelengths away from any other scattering structures such as buildings or trees.

The unique observation points were strategically chosen at 3m and 10m lateral distances from the front tip of the LP antenna. As stated in Chapter 2, in the model the lateral distance was adjusted back from the tip of the LP to account for the active region on the LP. At the 3m range measurements were taken at heights in half meter increments from 1m to 4m, and at the 10m range measurement heights were from 1m up to 5.5m. These height ranges are those recommended for standard OATS testing [10]. At each of these unique points, measurements were taken for all of the frequencies of interest. The entire set of measurements was duplicated with the LP antenna in both the vertical and horizontal orientations. This setup is shown in Figure 3.15.

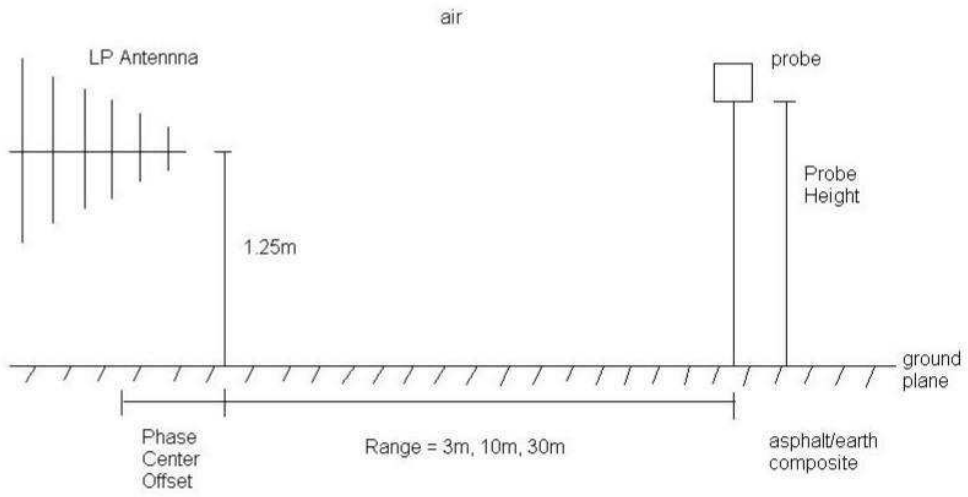

Figure 3.15: Illustration of the Setup for Obtaining Measurements

3.4 Observations on the Self Consistency of the Model

Before discussing the comparison of the experimentally measured fields to the results from the mathematical model, it was deemed necessary to establish some self-consistency within the model to determine if its results seemed reasonable or not. The methods that were employed in evaluating this self-consistency were different for vertical and horizontal polarization. The 10m range was chosen when using these methods due to the fact that this distance is far enough to be considered in the far field. For this LP, the far zone may be determined to be 5m. This maximum distance is related to wavelength and height of the source antenna above the ground [12].

The vertically polarized case is considered first. The approach for this polarization revolves around using the concept of the Brewster's angle which is defined by Equation (3.1) [7]:

$$\tan^{-1}\sqrt{\varepsilon_r} \tag{3.1}$$

where ε_r is the relative permittivity of the ground.

For the vertical polarization, Brewster's angle is defined as the angle at which all of the radiated energy hitting the ground plane is absorbed resulting in no reflection. From this angle one can calculate a specific height at a given distance that corresponds to this angle. At this height, it is assumed that the total field is very close to the direct field only since the contribution from the reflected field is negligible which means the field is essentially what it would be in free space. Table 3.1 shows the calculated so called "Brewster Heights" for each frequency in the 10m range.

Frequency (MHz)	Distance from Effective Radiating Dipole (m)	Brewster Height (m)
100	11.83	3.58
150	11.1	3.28
200	10.86	3.18
250	10.67	3.11
300	10.59	3.07
350	10.45	3.02
400	10.39	2.99

Table 3.1: Heights Corresponding to the Brewster Angle at 10m Range

With these calculations one is now able to check the model results at these specific heights to the fields that would be expected from a dipole in free space. To determine the electric field in the far zone from a dipole in free space, one can use Equation (3.2) shown below.

$$E = \frac{5.47}{R}\sqrt{P_t G_t} \tag{3.2}$$

where R is the distance from the dipole to the observation point, P_t is the power transmitted from the dipole, and G_t is the gain of the dipole.

Comparing the fields from this equation to the results from the model yielded reasonable results.

The next step was to check the model for consistency for the horizontally polarized case. Since the Brewster's angle does not apply to this polarization, a different approach was utilized. Considering the horizontal case, one knows that when the radiated field hits the ground, it undergoes a sign change. Also, it is observed that every half-wavelength traveled the field undergoes a sign change. Using this logic, one can calculate a height at a given range for which the reflected field travels a path that is a half-wavelength longer than the direct field. Then these two fields (direct and reflected) will completely add. This means that at this certain height the field from the dipole over a ground plane should be at a maximum (constructive interference) and should be roughly double the direct field. Table 3.2 shows these so called "half-wavelength heights" for each frequency at the 10m range.

Frequency (MHz)	Distance from Effective Radiating Dipole (m)	Height (m)
100	11.83	8.80
150	11.1	4.90
200	10.86	3.44
250	10.67	2.67
300	10.59	2.20
350	10.45	1.83
400	10.39	1.59

Table 3.2: Heights Corresponding to the Maximum Field for the Horizontal Polarization

After calculating these heights, the resulting measured fields are compared to the results of the model. While it can be seen that the fields at these heights are close to the maximum, they are not exactly correct. Looking at the plots there seems to be a trend that as frequency increases one observes a closer correlation between these heights and the maximum field. This observation and the inconsistencies observed may be due to the fact that in calculating these heights, the dipole was approximated as being located at its center point. In reality the dipole is a distributed source and radiates energy throughout its entire length. As frequency increases, the

resonant dipole length decreases which would make the approximation of the location of the radiation occurring at the center point more accurate.

While checking the model for self-consistency, it was also desired to find a way to relate the vertical and horizontal measured field amplitude to the similar cases of the model. From analysis of the vertical polarization results, it was determined that the field at the so-called "Brewster heights" should be roughly equal to the direct field. For the other test of the horizontal polarization, it was determined that fields at the "half-wavelength heights" were approximately equal to twice the direct field. Therefore, these "half-wavelength height" fields should be roughly twice the "Brewster height" fields that were calculated for each given frequency. Comparing these it is observed that the "half-wavelength height" fields were not quite twice but in the range of 1.5 to 1.7 times more than the corresponding "Brewster height" fields. This can be attributed to the fact that for the horizontal polarization, a ε_r=6, and the angle of incidence for reflection at the 10m distance, one will not get a reflection coefficient is equal to -1. From the model these values were observed to be in the -0.5 to -0.7 range. This means the field at the "half-wavelength height" will be slightly less than double the direct field.

3.5 Matching Measured Data and Model Results

After proving the model's self-consistency, the next task was to directly compare the model results to the measured data. One issue that had to be considered was that the measured data was taken with an emphasis on dynamic range of the electric field probes. The objective when taking the measurements was to adjust the radiated power to give a maximum field within the limits of the available RF power amplifiers. These radiated powers and fields are shown in Tables 3.3-3.6.

	100 MHz		150 MHz		200 MHz		250 MHz	
Height(m)	Power (W)	E (V/m)	Power (W)	E (V/m)	Power (W)	E (V/m)	Power (W)	E (V/m)
1	295.45	45.1	180.41	49.9	110.70	50.1	82.24	49.8
1.5	220.06	49.9	149.70	50.3	113.65	50.3	165.58	50.3
2	156.90	49.5	202.16	49.8	123.66	50.0	240.69	44.9
2.5	167.76	49.8	213.03	49.9	265.57	30.0	142.55	50.0
3	203.08	49.8	225.19	49.8	216.69	39.9	93.76	50.2
3.5	268.29	49.9	236.70	49.8	262.62	50.0	106.91	49.9
4	296.13	45.1	271.89	50.1	245.55	50.1	203.41	50.0

	300 MHz		350 MHz		400 MHz	
Height(m)	Power (W)	E (V/m)	Power (W)	E (V/m)	Power (W)	E (V/m)
1	130.52	50.1	248.86	40.0	212.09	25.0
1.5	241.80	40.1	250.80	45.0	265.57	35.0
2	127.92	49.9	82.31	50.1	85.93	49.8
2.5	117.00	50.2	132.66	50.0	101.47	50.2
3	92.04	50.0	136.54	50.2	139.41	49.8
3.5	164.84	50.1	198.03	39.9	224.89	44.9
4	194.48	25.0	230.47	44.8	202.49	50.0

Table 3.3: Radiated Powers and Fields for Horizontal Polarization at 3m Distance

	100 MHz		150 MHz		200 MHz		250 MHz	
Height(m)	Power (W)	E (V/m)	Power (W)	E (V/m)	Power (W)	E (V/m)	Power (W)	E (V/m)
1	87.62	49.9	60.14	49.9	40.63	50.1	28.51	50.0
1.5	99.84	49.6	47.98	50.1	38.27	50.0	14.26	49.9
2	320.58	45.3	245.66	50.0	263.80	44.9	138.17	49.9
2.5	302.25	39.8	246.30	50.0	263.80	44.9	216.02	49.8
3	282.55	34.8	262.29	44.9	183.72	35.0	226.99	40.1
3.5	269.64	29.9	312.19	40.0	146.62	25.0	201.77	29.9
4	221.42	24.9	239.26	30.0	148.98	19.9	211.09	25.0

	300 MHz		350 MHz		400 MHz	
Height(m)	Power (W)	E (V/m)	Power (W)	E (V/m)	Power (W)	E (V/m)
1	10.40	49.7	11.62	50.0	49.37	49.8
1.5	6.24	49.8	13.07	49.9	51.19	50.3
2	142.48	50.2	196.57	39.9	112.90	50.3
2.5	254.80	50.1	203.35	50.1	209.80	49.9
3	244.40	45.0	195.12	39.9	181.92	39.9
3.5	251.68	35.0	221.27	29.9	232.20	30.0
4	212.68	24.9	146.70	14.9	202.49	20.1

Table 3.4: Radiated Powers and Fields for Vertical Polarization at 3m Distance

	100 MHz		150 MHz		200 MHz		250 MHz	
Height(m)	Power (W)	E (V/m)	Power (W)	E (V/m)	Power (W)	E (V/m)	Power (W)	E (V/m)
1	287.98	10.0	166.97	10.0	216.11	15.0	222.60	20.0
1.5	154.18	10.0	215.59	15.0	220.23	20.0	211.63	25.0
2	357.94	20.0	241.82	20.0	246.14	30.0	218.76	40.1
2.5	325.34	20.0	173.37	20.0	223.76	25.1	234.11	39.9
3	223.46	20.0	277.64	30.0	172.53	29.8	232.47	49.9
3.5	284.59	25.0	273.17	35.1	230.24	35.0	225.89	35.0
4	234.33	25.0	268.69	35.0	237.30	29.9	191.90	20.0
4.5	340.28	30.0	240.54	30.0	215.52	25.0	161.74	20.0
5	306.32	30.1	293.00	29.9	170.76	20.1	197.93	14.9
5.5	355.22	30.0	236.06	25.0	133.08	15.0	169.42	5.0

	300 MHz		350 MHz		400 MHz	
Height(m)	Power (W)	E (V/m)	Power (W)	E (V/m)	Power (W)	E (V/m)
1	249.60	25.0	168.98	20.0	130.27	10.0
1.5	148.20	25.1	176.24	25.1	126.16	10.1
2	244.40	40.1	256.13	35.0	239.97	35.2
2.5	219.96	45.0	210.61	39.9	169.12	25.0
3	208.52	40.1	157.36	15.0	96.45	5.0
3.5	130.00	10.0	209.16	15.0	140.33	15.0
4	187.72	15.1	170.43	10.0	127.98	15.1
4.5	247.52	7.5	168.49	20.0	163.64	25.0
5	237.12	15.0	251.77	30.0	160.90	20.0
5.5	262.08	25.0	246.93	25.0	158.15	20.0

Table 3.5: Radiated Powers and Fields for Horizontal Polarization at 10m Distance

	100 MHz		150 MHz		200 MHz		250 MHz	
Height(m)	Power (W)	E (V/m)	Power (W)	E (V/m)	Power (W)	E (V/m)	Power (W)	E (V/m)
1	290.70	25.0	330.74	34.9	249.67	45.0	168.32	50.1
1.5	363.37	30.0	312.83	39.9	239.66	45.1	172.71	49.9
2	198.33	10.0	278.28	19.9	147.21	15.0	127.75	15.0
2.5	350.47	15.0	243.74	20.0	142.50	15.0	123.36	15.0
3	329.41	15.0	236.06	20.0	153.10	15.0	226.44	20.0
3.5	292.06	14.9	224.55	20.0	158.40	15.0	219.31	20.0
4	337.56	15.0	252.06	20.0	236.72	15.0	210.54	20.0
4.5	352.51	15.0	281.48	20.0	100.10	10.0	203.41	20.0
5	376.96	15.0	314.75	19.9	105.40	10.0	217.12	20.0
5.5	156.90	10.0	207.91	15.0	121.89	10.0	149.13	15.0

	300 MHz		350 MHz		400 MHz	
Height(m)	Power (W)	E (V/m)	Power (W)	E (V/m)	Power (W)	E (V/m)
1	137.80	49.9	220.30	50.0	193.35	35.0
1.5	125.32	49.1	107.49	50.1	207.52	49.4
2	247.00	20.0	188.34	25.1	198.38	25.1
2.5	263.12	25.0	170.91	24.9	220.32	25.0
3	211.12	25.0	174.30	25.0	207.06	20.1
3.5	197.60	25.0	225.14	25.1	138.04	15.0
4	212.68	25.0	235.79	20.0	180.09	15.0
4.5	170.04	20.0	202.38	15.0	160.44	15.0
5	262.08	20.0	251.77	15.1	161.35	15.0
5.5	256.36	15.0	134.12	10.0	184.21	15.0

Table 3.6: Radiated Powers and Fields for Vertical Polarization at 10m Distance

In order to compare the measured and modeled data, these fields needed to be normalized to the same radiated power. It was decided to normalize the fields to a constant effective radiated power of 100 W for all cases. These normalized fields are shown in Tables 3.7-3.10 and are the field values represented on the comparison plots presented at the end of the chapter.

	100MHz	150MHz	200MHz	250MHz	300MHz	350MHz	400MHz
Height(m)	E (V/m)	E (V/m)	E (V/m)	E (V/m)	E (V/m)	E (V/m)	E (V/m)
1	26.24	37.2	47.6	54.9	43.9	25.4	17.2
1.5	33.64	41.1	47.2	39.1	25.8	28.4	21.5
2	39.52	35.0	45.0	28.9	44.1	55.2	53.7
2.5	38.45	34.2	18.4	41.9	46.4	43.4	49.8
3	34.95	33.2	27.1	51.8	52.1	43.0	42.2
3.5	30.47	32.4	30.9	48.3	39.0	28.4	29.9
4	26.21	30.4	32.0	35.1	17.9	29.5	35.1

Table 3.7: Normalized Field Values for Horizontal Polarization at 3m Distance

	100MHz	150MHz	200MHz	250MHz	300MHz	350MHz	400MHz
Height(m)	E (V/m)	E (V/m)	E (V/m)	E (V/m)	E (V/m)	E (V/m)	E (V/m)
1	53.31	64.3	78.6	93.6	154.1	146.7	70.9
1.5	49.64	72.3	80.8	132.2	199.4	138.0	70.3
2	25.30	31.9	27.6	42.5	42.1	28.5	47.3
2.5	22.89	31.9	27.6	33.9	31.4	35.1	34.5
3	20.70	27.7	25.8	26.6	28.8	28.6	29.6
3.5	18.21	22.6	20.6	21.0	22.1	20.1	19.7
4	16.73	19.4	16.3	17.2	17.1	12.3	14.1

Table 3.8: Normalized Field Values for Vertical Polarization at 3m Distance

	100MHz	150MHz	200MHz	250MHz	300MHz	350MHz	400MHz
Height(m)	E (V/m)	E (V/m)	E (V/m)	E (V/m)	E (V/m)	E (V/m)	E (V/m)
1	5.90	7.73	10.20	36.67	15.85	15.35	8.75
1.5	8.08	10.21	13.48	42.18	20.59	18.89	8.95
2	10.55	12.86	19.14	53.37	25.65	21.87	22.72
2.5	11.08	15.17	16.75	42.99	30.34	27.49	19.25
3	13.35	17.98	22.69	53.50	27.77	11.98	5.10
3.5	14.83	21.24	23.07	50.05	8.73	10.36	12.65
4	16.31	21.35	19.42	42.02	10.99	7.68	13.32
4.5	16.24	19.34	17.01	38.67	4.75	15.42	19.53
5	17.19	17.48	15.36	36.74	9.73	18.93	15.80
5.5	15.92	16.28	12.99	32.20	15.44	15.92	15.86

Table 3.9: Normalized Field Values for Horizontal Polarization at 10m Distance

	100MHz	150MHz	200MHz	250MHz	300MHz	350MHz	400MHz
Height(m)	E (V/m)	E (V/m)	E (V/m)	E (V/m)	E (V/m)	E (V/m)	E (V/m)
1	14.66	19.19	28.48	38.62	42.51	33.69	25.17
1.5	15.74	22.56	29.13	37.97	43.86	48.32	34.29
2	7.09	11.94	12.34	13.26	12.75	18.27	17.81
2.5	8.02	12.80	12.56	13.49	15.40	19.04	16.82
3	8.24	12.98	12.13	13.27	17.23	18.92	13.93
3.5	8.74	13.33	11.91	13.52	17.78	16.70	12.78
4	8.18	12.58	9.76	13.78	17.12	13.01	11.20
4.5	7.98	11.92	9.99	14.04	15.37	10.57	11.81
5	7.73	11.23	9.75	13.59	12.34	9.50	11.79
5.5	7.96	10.38	9.05	12.28	9.37	8.64	11.06

Table 3.10: Normalized Field Values for Vertical Polarization at 10m Distance

With the measured data now in the normalized form one can adjust the model results. A final step was to decide an appropriate driving voltage for the dipole in the model. The first approach was basically trial and error to most closely match the measurements. All calculations were performed at the 10m range. The reason for doing this was that for the 3m range at 100 MHz, the separation distance is roughly one wavelength. This separation distance is too close to expect accurate results due to effects of the various interactions between the radiating antenna, its support structure, the receiving antenna (probe), and its support structure. After adjusting the gap voltage and plotting the model results against the measured results, it was finally arrived at a value of 180 V to drive the dipole for all cases.

With a gap drive voltage determined, the question to answer is whether these results are reasonable or not. One way of answering this is to determine the inferred gain built into this model for the dipole and check this against the design gain of the actual LP antenna.

Consider the 250 MHz case for vertical polarization. Look at the field at the previously calculated “Brewster height” of 3.11m. Examining the scaled measurement values for the LP antenna radiating 100 W of power, one finds the field at this height to be approximately 13 V/m.

From previous results of the model when driven with 1V gap voltage, it is observed that a current of 13.92 mA is produced at the driving point of the dipole. Plugging this drive voltage and current into Equation (3.3), one arrives at a radiation resistance of 71.8 ohms. This resistance is very typical of a resonant dipole.

$$P = VI = I^2 R_{rad} = \frac{V^2}{R_{rad}} \tag{3.3}$$

where P is the radiated power, V is the driving gap voltage, I is the current on the dipole, and R_{rad} is the radiation resistance of the dipole.

Using Equation 3.3 one can calculate the effective radiated power from the dipole model with a drive voltage of 180V and radiation resistance of 71.8 ohms. Using these values, one finds the power radiated to be equivalent to 451.3 W. Finally, using Equation (3.4), one can see that the inferred gain is a ratio of this calculated power to the scaled value of radiated power from the measurements of 100W. For this particular case one finds the inferred gain to be 4.51 or 6.54 dB.

$$G_{\text{inf } erred} = \frac{P_{rad}}{100} \tag{3.4}$$

This result seems to be very reasonable since the nominal design gain for this LP antenna was roughly 7 dB. More cases at other frequencies were tested in this manner and it was found that they all yielded similar results. This gives an independent confirmation that the chosen driving voltage for the model of 180V is reasonable.

One other point that cannot go unmentioned is the correlation of the normalized measured fields and the scaled model fields are in poor agreement for the measurement heights of 1m and 1.5m for the vertically polarized case. This lack of agreement is present for both the 3m and 10m ranges. This consistent lack of agreement resulted in confusion over the cause of it

and/or how to fix this problem. Addition data (not included in this thesis) were measured at similar observation points and frequencies with the radiating source being a Seavey commercial dual-polarized ridged horn. The data taken with this horn is being analyzed by other engineers at Redstone Arsenal, AL. From the data taken in front of the ridged horn, the fields also show unusual behavior for the two measurement heights of 1m and 1.5m for the vertically polarized case. For heights above 1.5m, the data yields smooth and predictable values for the fields. The same measurement techniques were used to obtain both sets of radiated field data.

Both data sets show this field "anomaly" for the 1m and 1.5m heights. For both the LP and ridged horn sets of data, field data at these two heights were measured with the probe located on the top of a wooden tripod with a circular "metallic" head. Fields for all heights above 1.5m were measured with the field probe positioned on a dielectric arm that could be slid up and down an 18 ft, 3.5 inch diameter PVC pipe.

Due to the fact that all data above 1.5m (for the LP and ridge horn) appears consistently smooth and predictable, one suspects that there may be unknown interaction between the tripod and the electric field probe.

CHAPTER 4

ISSUES ASSOCIATED WITH FIELD EXTRAPOLATION OVER THE GROUND

4.1 Introduction

This chapter will address the issue of field extrapolation from one range to another. Section 4.2 introduces a commonly used approach to this problem. Section 4.3 uses this technique to calculate extrapolation factors using the measured data for all cases. Lastly, Section 4.4 presents the results of this extrapolation along with conclusions drawn from the measured and modeled data.

4.2 Extrapolation Methods

The task of extrapolating fields from one range to another is a difficult and widely debated problem. A common procedure used in extrapolation, which is even required in some test guidelines, is to use the far field term of 1/R where R is the distance from the source to the observation point. Using this method, extrapolation from 3m to 10m should produce a 10.46dB reduction in field strength and 10m to 30m a 9.54dB reduction. While this method is widely used, there are numerous papers and sources that show this approach has a large range of errors [9].

4.3 Extrapolation of Measured Fields

Tables 4.1 and 4.2 highlight extrapolation results scaling the measured data using the 1/R method discussed in the previous section. The measured data was used to compare the radiated fields at 3m and 10m at measurement heights of 1m to 4m. Figures 4.1 to 4.4 display the extrapolation factor for both the 3m to 10m range and the 10m to 30m range. There was no measured data for the 30m range, so the values from the model were used at each measurement height.

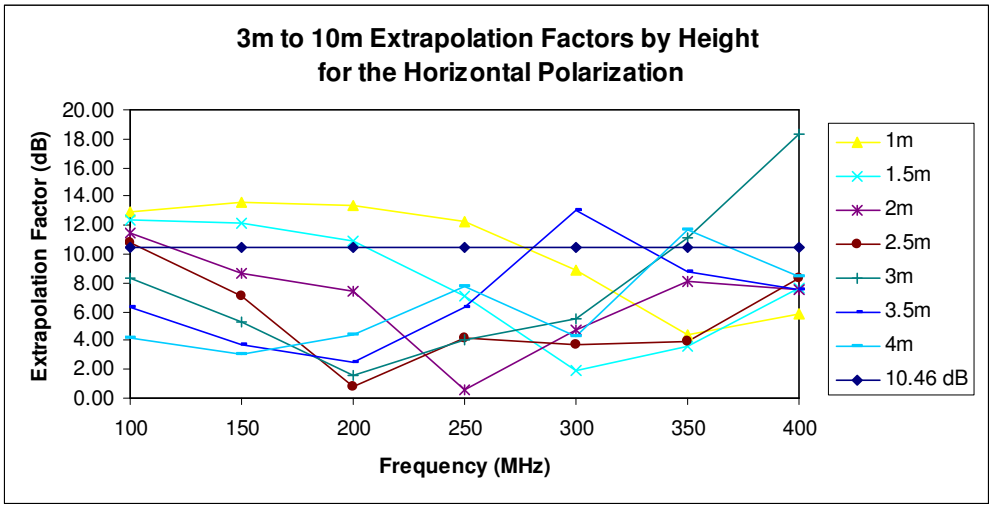

Figure 4.1: Extrapolation Factor Plot for 3m to 10m for Horizontal Polarization

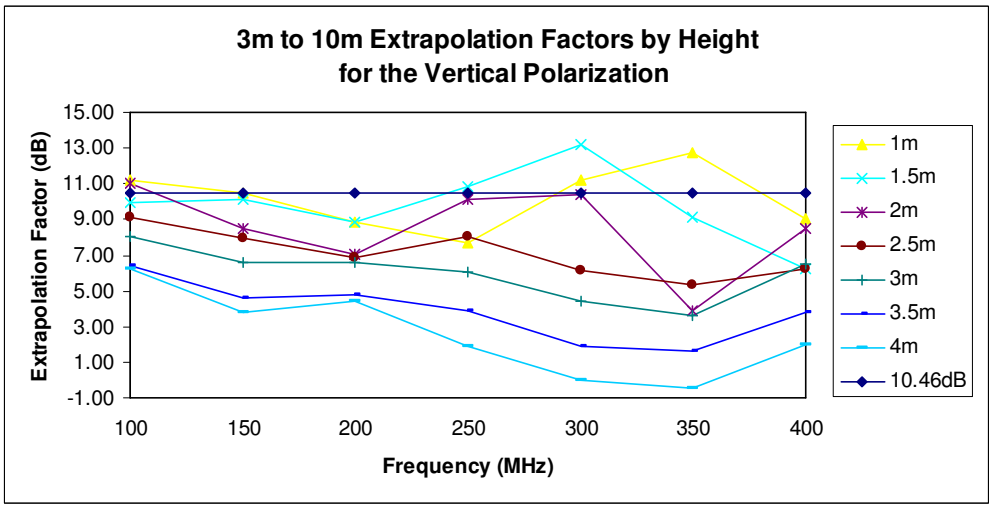

Figure 4.2: Extrapolation Factor Plot for 3m to 10m for Vertical Polarization

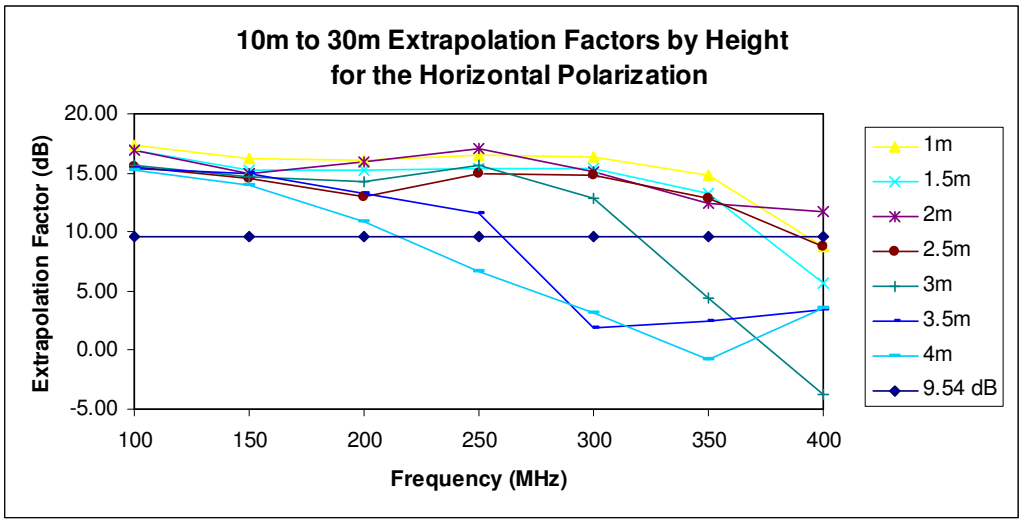

Figure 4.3: Extrapolation Factor Plot for 10m to 30m for Horizontal Polarization

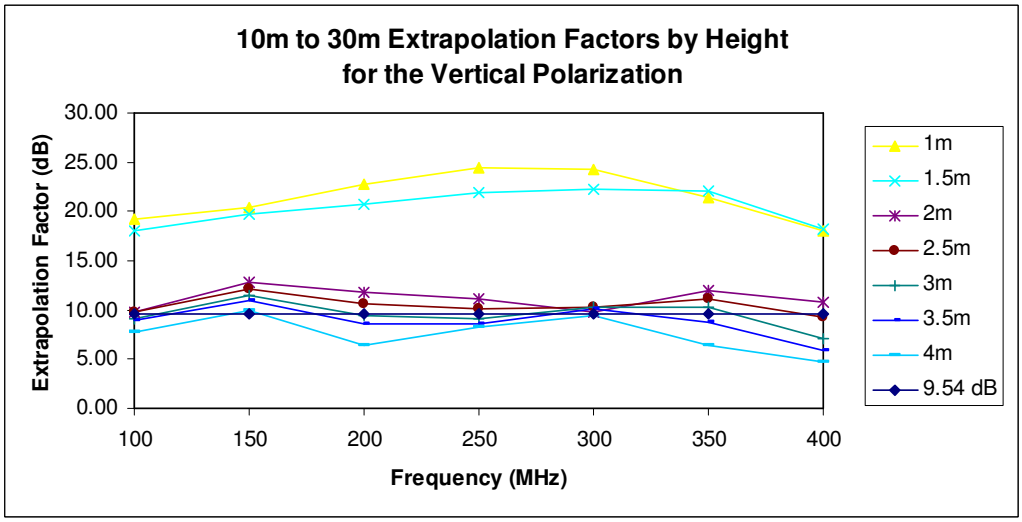

Figure 4.4: Extrapolation Factor Plot for 10m to 30m for Vertical Polarization

	Field Reduction (dB)						
Height(m)	100MHz	150MHz	200MHz	250MHz	300MHz	350MHz	400MHz
1	12.96	13.63	13.39	12.27	8.84	4.36	5.85
1.5	12.39	12.10	10.88	7.13	1.95	3.55	7.61
2	11.47	8.70	7.42	0.57	4.71	8.05	7.47
2.5	10.81	7.06	0.83	4.11	3.69	3.97	8.26
3	8.36	5.32	1.55	4.00	5.47	11.09	18.35
3.5	6.26	3.66	2.53	6.33	13.01	8.75	7.48
4	4.12	3.06	4.33	7.71	4.23	11.69	8.42

Table 4.1 Measured Field Extrapolation Results from 3m to 10m
for the Horizontal Polarization

	Field Reduction (dB)						
Height(m)	100MHz	150MHz	200MHz	250MHz	300MHz	350MHz	400MHz
1	11.21	10.51	8.82	7.69	11.19	12.78	8.99
1.5	9.98	10.12	8.86	10.83	13.15	9.12	6.24
2	11.05	8.54	7.01	10.11	10.37	3.85	8.49
2.5	9.11	7.92	6.85	8.00	6.18	5.32	6.23
3	8.01	6.59	6.56	6.04	4.46	3.58	6.54
3.5	6.38	4.60	4.78	3.85	1.88	1.61	3.76
4	6.22	3.76	4.46	1.93	-0.02	-0.47	2.00

Table 4.2 Measured Field Extrapolation Results from 3m to 10m
for the Vertical Polarization

4.4 Conclusions

Looking at Tables 4.1 and 4.2 as well as Figures 4.1 to 4.4, it can be seen that the extrapolation values vary greatly with height and frequency from the nominal value of 10.46 dB for extrapolation from 3m to 10m and 9.54 dB for extrapolation from 10m to 30m. This indicates that the extrapolation factor is not frequency independent. From the results it can also be seen that these factors must also be height dependent including not only the height of the measurement but also the height of the source. Clearly it can be seen that the simple 1/R far field term is not adequate for field extrapolation.

CHAPTER 5

CONCLUSIONS

In this thesis, a MoM model was developed to represent and calculate radiated emissions from a log periodic antenna over an actual ground. Results from the model were then compared with experimentally obtained measurement previously performed in an OATS environment over actual ground without the presence of a conducting ground screen or grid. The results show a strong correlation between the model calculations and the measured values. Further analysis of these results also serve to validate the model along with demonstrating its self-consistency.

Finally, the results for extrapolation were calculated and compared to the widely used extrapolation factor of 1/R. The comparison clearly shows extrapolation to be dependant on a variety of factors such as frequency and height of the source as well as height of the observation point. Extrapolation factors varied significantly from the standard factor 1/R and these data serve to validate that this simple term in not sufficient when extrapolating radiated emissions from one range to another.

With the measurements having previously been completed, it was not possible to go back and re-measure the cases which deviated from the model results. This would have been very useful toward further proving the validity of the model.

Future work might involve expanding on the model to more accurately represent the LP antenna as well as incorporating an actual ground plane into the model. This might provide an

even more accurate tool for tackling the very complicated problem of extrapolating radiated emissions over a ground plane.

REFERENCES

[1] W. C. Gibson, *The Method of Moments in Electromagnetics*. Boca Raton: Chapman and Hall/CRC, 2008.

[2] S. M. Rao, "ELEC 7310 Computational Electromagnetics I Class Notes". Auburn University, Spring 2009.

[3] R. F. Harrington, *Time-Harmonic Electromagnetic Fields*. New York: IEEE Press, 2001.

[4] W. L. Stutzman and G. A. Thiele, *Antenna Theory and Design, 2nd Edition*. New York: John Wiley and Sons, 1998.

[5] K. Rong, S. Donglin, and Y Zhengguang, "Research of Phase Center of Log-periodic Dipole Antenna". IEEE International Symposium on Microwave, Antenna, Propagation, and EMC Technologies for Wireless Communications. 2007.

[6] T. Saarenketo, "Measuring Electromagnetic Properties of Asphalt for Pavement Quality Control and Defect Mapping". http://vgwww.vegagerdin.is/nvf33.nsf/7c5e95b3edddb9e980256f620045f483/6423655ed26a5bd400256de90031ecaf/$FILE/Asphalt_electromagnetics_TimoS_030603.pdf, viewed October 2009.

[7] S. Wentworth, *Fundamentals of Electromagnetics with Engineering Applications.* New York: John Wiley and Sons, 2004.

[8] L. Riggs and T. Shumpert, "Trajectories of the Singularities of a Thin Wire Scatterer Parallel to Lossy Ground'. *IEEE Transactions on Antennas and Propagation*, Vol. AP-27 No. 6, pg. 864-868, November 1979.

[9] H. Garn, E. Zink, and R. Kremser, "Problems with Radiated-Emission Testing at 3m Distance According to CISPR 11 and CISPR 22". IEEE International Symposium on Electromagnetic Compatibility. 1993.

[10] F. Gisin, Z. Pantic-Tanner, "Analysis of the Measurement Uncertainty Associated with 1/R Extrapolation of Radiated Emission Measurements on an Open Air Test Site (OATS)". IEEE International Symposium on Electromagnetic Compatibility. 1998.

[11] C. Paul, *Introduction to Electromagnetic Compatibility*. New Jersey: John Wiley and Sons, 2006.

[12] L. Hemming and R. Heaton, "Antenna Gain Calibration on a Ground Reflection Range". *IEEE Transactions on Antennas and Propagation*, Vol. 21 No. 4, pg. 532-538, July 1973.